Online design of PCB UHF/RFID antennas Page 6

EDN europe

contents
September 2013

DEPARTMENTS & COLUMNS

DESIGNIDEAS

pulse

EDN europe

CONTACTS

PUBLISHER
André Rousselot
+32 27400053
andre.rousselot@eetimes.be

EDITOR-IN-CHIEF
Graham Prophet
+44 7733 457432
edn-editor@eetimes.be

Patrick Mannion
Brand Director EDN Worldwide

CIRCULATION & FINANCE
Luc Desimpel
luc.desimpel@eetimes.be

ADVERTISING PRODUCTION & REPRINTS
Lydia Gijsegom
lydia.gijsegom@eetimes.be

ART MANAGER
Jean-Paul Speliers

ACCOUNTING
Ricardo Pinto Ferreira

SALES CONTACTS

Europe

Daniel Cardon
France, Spain, Portugal
+33 688 27 06 35
cardon.d@gmail.com

Nadia Liefsoens
Belgium
+32-11-224 397
n.liefsoens@fivemedia.be

Nick Walker
UK, Ireland, Israel,
The Netherlands
+44 (0) 1442 864191
nickjwalker@btinternet.com

Victoria & Norbert Hufmann
Germany PLZ 0-3, 60-65, 8-9,
Austria, Eastern Europe
+49 911 93 97 64 42
sales@hufmann.info

Armin Wezel
Germany PLZ 4-5
+49 (0) 30 37445104
armin@eurokom-media.de

Ralf Stegmann
Germany PLZ 66-69, 7
+49 7131 9234-0
r.stegmann@x-media.net

Monika Ailinger
Switzerland
+41-41-850 4424
m.ailinger@marcomedia.ch

Ferruccio Silvera
Italy
+39-02-284 6716
info@silvera.it

Colm Barry & Jeff Draycott
Scandinavia
+46-40-41 41 78
jeff.draycott@womp-int.com
colm.barry@telia.com

USA & Canada

Todd A. Bria
West
+1 831 477 2075
tbria@globalmediasales.com

Jim Lees
PA, NJ & NY
+1-610-626 0540
jim@leesmedia.com

Steve Priessman
East, Midwest,
South Central
& Canada
+1-630-420 8744
steve@stevenpriessman.com

Lesley Harmoning
East, Midwest,
South Central
& Canada
+1-218.686.6438
lesleyharmoning@gmail.com

Asia

Masaya Ishida
Japan
+81-3-6824-9386
MIshida@mx.itmedia.co.jp

Bennie Hui
Asian Sources Publications
Hong Kong
+852 2831 2775
bennie@globalsources.com

THROUGH A GLASS

Among the lower-budget US TV-show imports that populate the out-of prime-time corners of the programming schedule, there's one called "Person of Interest". Its basic premise is built on melding several real-world trends and extrapolating a fictional result. It feeds, to some extent, on the prevalence in our cities of widespread CCTV surveillance, and it also embraces the concept of "predictive policing" in which law-enforcement bodies carry out statistical analyses of the location, timing and prevalence of crime to allocate police resources in the places that crimes are most likely to occur. The (somewhat preposterous) fiction is that a massive computing resource can identify individual people who are about to be involved in a crime – the scriptwriters' degree of freedom is that "the machine" doesn't know what that crime will be or when it will happen.

This programme came to mind recently when I was reading some of the coverage of trials and public reaction to the introduction of Google Glass. In EDN Europe, we recently carried a "Teardown" article on Google Glass, which is available here. Unless you have been on an extended retreat, you cannot have missed coverage of Google Glass, and know that it is a spectacle-frame headset with camera, projected virtual-screen display and voice-operated command set. Users/wearers can access information and take pictures on-the-fly and on the move, with spoken commands. Naturally, there has been a great deal of discussion about the social context in which such a device will be used. When is it polite/acceptable to have such a product switched on, or to capture images with it? If you have one, is it appropriate for me to ask that you turn it off/remove it while you are talking to me? - Or is that mere paranoia? Many such questions have been posed, as the briefest of searches (via Google, of course) will reveal. Reaction of enthusiasts has, not for the first time, displayed an interesting, perhaps wilful, avoidance of one of the essential features of the computing-consumer-gadgetry scene: namely, its rate of progress. Those reactions have been to point out that Glass doesn't capture images all the time, it doesn't stream to the web, you can see when it's taking a picture – what's the problem?

The problem, if there is one, may lie a couple of product generations out; imagine a few more steps down, in power consumption and up, in computing density – maybe then you could have a device that would indeed stream constant video to the network. What would Google do with all that data? That, perhaps, is the easy question – the default setting is to archive it all in data centres and find a way of "monetising" it. It's easy to speculate that by linking it with facial recognition and the social networking databases you could have instant recognition and read-out on anyone you came in contact with. Which is where the premise of the TV show comes to mind; if a significant number of citizens were to be capturing live data all the time, the idea that "the system" could know where everyone is, and what they are doing, all the time, begins to look a little less preposterous. If such a resource ever came into existence, it is hard to imagine that Governments and their Agencies would restrain themselves from accessing it – but I'll leave that particular strain of thinking to the conspiracy theorists.

The thought that I'd like to leave you with is this; if there is anything we have to monitor as this technology evolves, it's perhaps not the gadgetry and its capabilities, but ourselves. I refer to the phenomenon variously called "creeping normalcy" or "altered perspective" - the way in which something which was outrageous yesterday transitions, un-noticed, through some process of acceptance and becomes unremarkable tomorrow or even, today. Glass' advocates may not have to solve the social-context issues; our attitudes could do it for them. The precedents are everywhere; information that previous generations regarded as entirely private, we now post freely on social media. (Or, more accurately, some of us do.)

And that's how it may be in this case; in a few years (or just months?) you may aim your Glass, or its descendent, at me. The social rules of that time may dictate that I will not be entitled to see that as an intrusion: instead, when your readout says, "no data on this person", I will be the one who is violating social norms, by declining to provide a complete online profile, ready for you to download. Personally, if this scenario does come to pass, I can live with that burden!

pulse

NXP offers on-line tool for UHF PCB antenna design

This design tool helps electronics manufacturers implement RFID technology; manufacturers wanting to embed RFID technology in their products are now able to do so without needing extensive UHF antenna design experience. The RFID – PCB online software Antenna Designer tool helps implement antennas on a printed circuit board in the UHF frequency range (840-960 MHz). UHF antenna design is more complex than a typical HF antenna design and needs an expert understanding of the electronic design constraints, NXP notes. With the RFID – PCB Antenna Designer you can simply input parameters, such as space available on the PCB, target performance, board materials, and target frequency range in the region of application, to receive a turnkey UHF antenna design for a specific application. Additionally, the tool offers a comprehensive overview of all the features of the UCODE series of RFID transceiver chips, enabling you to select the right UCODE product for an application.

The RFID – PCB Antenna Designer tool has a user-friendly interface to help non-RFID experts design high performance antennas and generates customised and application-specific antenna designs; it has been produced with support from leading
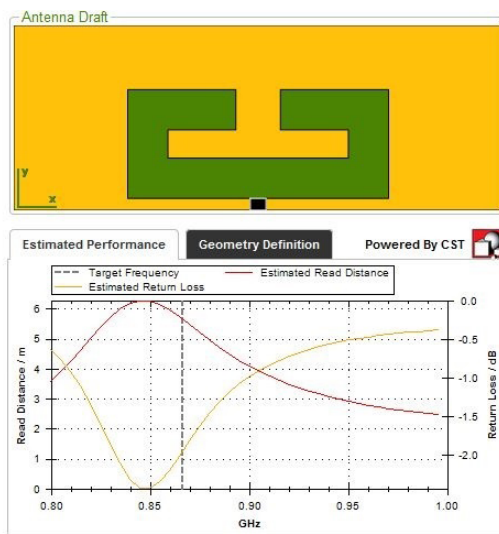
The Antenna Designer tool gives both geometric details to lay out an antenna, and graphical feedback on its predicted performance.

engineering companies, CST (Computer Simulation Technology) and Transim: the online design tool is available to use now. CST develops high performance software for the simulation of electromagnetic fields in all frequency bands: Transim delivers innovative cloud application engineering solutions for online design support in the electronics industry.

The online RFID – PCB Antenna Designer tool currently supports the following devices: UCODE I2C in an SOT902 package; UCODE G2iL in an SOT886 package; and UCODE G2iM in an SOT886 package.

"For customers wanting the benefits of using RFID technology in their products the challenge of designing a good UHF antenna on their PCB board can often be quite daunting. We are helping customers overcome this hurdle with our latest online offering, the Antenna Designer tool. Created to ease design problems, the tool delivers a full turnkey UHF antenna solution quickly with an outstanding level of performance," said Mohammed Chemloul, customer application support (CAS) manager, business unit Identification, NXP Semiconductors.

NXP; http://nxp.transim.com/rfid/design.aspx#icSelection and http://nxp-rfid.com/

Maxim to buy integrated-power-silicon supplier Volterra

Maxim Integrated Products has announced it has agreed to acquire Volterra Semiconductor: Volterra is a maker of high-current, high-performance, and high-density power management silicon. The company develops highly integrated solutions primarily for the enterprise, cloud computing, communications, and networking markets.

"Maxim Integrated is known for its highly integrated solutions. With Volterra, we will strengthen our position in the enterprise and communications markets," said Tunç Doluca, Maxim's President and Chief Executive Officer. "We add a very talented team and leading-edge proprietary technology in high-current power management solutions, which further diversifies our business model."

"This is an attractive transaction for our employees, customers, and investors," said Jeffrey Staszak, Volterra's President and

Chief Executive Officer. "The Volterra team will build upon Maxim's scale and market leadership to expand our ability to deliver innovative and differentiated products to our customers."

At $9 billion, power management is currently the largest and fastest-growing product segment in the analogue market, according to quoted by Maxim, from analyst Databeans. Maxim already offers a broad portfolio of products for power conversion: switching regulators, linear regulators, charge pumps, digital Point-of-Load (POL) converters, and Power Management Integrated Circuits (PMICs), primarily in medium-to-low current applications. Volterra's high-current technology expands the company's position in this [higher power] growing segment of the analogue market.

Maxim paid $605 million for Volterra ($23 per share, 55% over Volterra Semiconductor's closing share price on August 14, 2013), but gets $155 million cash that Volterra held, meaning the deal is worth a net $450 million.

NMaxim, www.maximintegrated.com
Volterra, www.Volterra.com

Source/measure unit gains touchscreen user interfaces

Keithley has produced an updated version of its current/voltage source/measure instruments (SMUs) that includes operation via a touchscreen graphical interface, and that also sees a number of specification upgrades. The introduction of touchscreen operation reflects trends in the wider market (with touch becoming the default user interface on many consumer products) but is also aimed at making the units more immediately usable by a range of non-T&M specialists, Keithley says.

Some of the enhanced low-level capabilities will be applicable to low-resistance measurements, for example in characterising connectors; verifying low circuit resistance can be critical in alternative energy installations, and once again, may be made by users who are specialist in fields other than electronic measurement.

The unit can provide, Keithley says, the capabilities of I-V systems, curve tracers, and semiconductor analysers at a fraction of their cost. The Model 2450 SourceMeter SMU Instrument combines intuitive touchscreen and icon-based control that novice SMU users can appreciate with the versatility that experienced users can make use of. You can select the source (current or voltage, source or sink) by dragging the appropriate icon on the screen, and connecting it in the same way, and set parameters and levels either on-screen or via an adjacent rotary control.

The Model 2450's operation is based on the company's "Touch, Test, Invent" design philosophy, which Keithley says reflects recent market changes, including shrinking product design/development cycles and fewer personnel devoted exclusively to test engineering tasks. At the same time, the profile of the typical instrument user has also evolved. In addition to electrical engineers, it now includes a growing number of non-engineers (such as electrochemists, physicists, materials scientists,

etc.) who need fast access to data but sometimes have limited training in electrical measurement. Younger engineers tend to be more software-oriented than hardware oriented, the company notes. To accommodate all of these market and user changes, the Model 2450 incorporates numerous ease-of-use features that ensure a faster "time-to-answer" than competitive solutions, including a context-sensitive help function, "Quickset" modes that speed instrument configuration, and on-screen graphing capabilities that quickly turn raw data into usable results.

The Model 2450 builds on the precision of both the Model 2400 SourceMeter SMU instrument and the newer Series 2600B System SourceMeter SMU. The

Keithley positions the 2450 as the first-available source-measure unit that has full touch-screen control.

Model 2450 combines a power supply, true current source, 6½-digit multimeter, electronic load, and trigger controller in one integrated, half-rack instrument. Features include;

- Full-colour, 5-in. touchscreen user interface.
- Extended measurement ranges with extended low current performance: the new low current (100 nA, 10 nA) and voltage (20 mV) ranges eliminate the need to add separate low-level instruments to a benchtop system. Back-panel triax cable connections eliminate the need for expensive cable adaptors, which can degrade low-level measurement performance.
- Built-in context-sensitive help function: help information is provided where it's

needed through the touchscreen, minimising the need to review a manual.
- Error and event logging: the touchscreen displays error messages and an event log to simplify diagnosing instrument errors.
- KickStart start-up software: this "no-programming" instrument control software simplifies taking and graphing data. For more complex analyses, data can be stored to disc, and then exported to Microsoft Excel or another software environment.
- Embedded Test Script Processor (TSP): a Test Script Processor embeds complete test programs into non-volatile memory within the instrument itself to provide higher test throughput by eliminating the GPIB traffic problems common to systems dependent on an external PC controller.
- TSP-Link inter-unit communication bus: unlike users of mainframe-based systems, Model 2450 users are not constrained by power or channel count limitations. TSP-Link connections support system expansion with multiple 2450s and other TSP instruments, including Series 2600B SMU instruments and the Model 3706A Switch/Multimeter. Up to 32 Model 2450 instruments can be linked for multi-point or multi-channel parallel test, under the direction of a master unit's TSP controller.
- PC connectivity and automation: Rear panel triax connectors, multiple instrument communication interfaces (GPIB, USB 2.0, and LXI/Ethernet), a D-sub 9-pin digital I/O port (for internal/external trigger signals and handler control), instrument interlock control, and TSP-Link jacks simplify configuring multi-instrument test setups.

The Model 2450 costs €4,535/£3,810; a version without a front panel designed for integration into automated systems is available for €4,283/£3,598.

Keithley; www.touchtestinvent.com / www.keithley.com

pulse

Solid-state relay reference design offers remote, wireless AC power switching

by Jean-Pierre Joosting

The remote power-switching design builds wireless controller and SSR into a standard power outlet – in this example, a US-format socket.

Zilog, now part of IXYS, has introduced its ZAURA Reference Design to expand its portfolio of digital wireless solutions that are aimed at industrial wireless connectivity in control and sensing, power metering applications, and for eliminating standby power consumption. This reference design integrates Zilog's ZAURA RF 868 MHz wireless module onto a current-sensing power SSR and is designed to showcase wireless control of an AC power SSR. The IXYS ICD power SSR, part number CPC1966, features AC zero-crossing detection to minimise surge currents and sine wave distortions. This reference design can be used as a basis for developing systems that can control a wide range of power products.

On its own, without the ZAURA RF wireless 868 MHz module attached, this design's Base Power Board functions as a development board to provide current to power the module and the switch. With the Module attached and controlled by a hand-held remote control device, RF communication can turn a load on and off. To demonstrate RF control, a hand-held ZAURA RF remote control device is also included with the reference design. Documentation supplied provides specifications and schematics, describes its software commands, and also provides a procedure for quickly getting started with development.

Zilog; www.zilog.com

Signal analysers gain improved phase-noise performance, sweep speed

Agilent Technologies recently announced greater core performance in two of its X-Series signal analysers, the midrange MXA and general-purpose EXA. Improvements in phase noise allow you to more precisely characterise the frequency stability of oscillators and synthesisers. The faster sweep speeds of these analysers accelerate searches for spurious signals in the testing of transmitters, active antenna arrays and power amplifiers.

In the MXA, phase noise has been improved by 10 dB or more for close-in and pedestal offset frequencies, providing an advantage of 7 dB over the closest instrument in the market, Agilent claims - phase-noise performance is a key factor in obtaining low and accurate error vector magnitude values for communication systems and devices. EXA phase-noise performance is up to 5 dB better across wide offset frequencies.

In manufacturing test, spur searches in wide spans at narrow resolution bandwidths have been slow and are often the cause of bottlenecks. The new "fast sweep" capability of these analysers is up to five times faster than that of competitive models, depending on resolution bandwidth. Faster sweeps improve measurement throughput and make it easier to check the spurious-free dynamic range of devices under test.

"The MXA enhancements are an important complement to our recently introduced options for 160-MHz analysis bandwidth and real-time spectrum analysis," according to Jim Curran, marketing manager of Agilent's Microwave Communications Division.

Agilent has also upgraded three of the measurement applications available for X-Series signal analysers. The N9069A noise figure measurement application now includes advanced features that support measurements of multistage converters, multipliers and dividers: N9080A (FDD) and N9082A (TDD) LTE measurement applications now support multimedia broadcast single-frequency network (MBSFN) signals with mixed cyclic-prefix subframe structures. This allows you to test physical multicast channels and MBSFN reference signals using virtually any subframe-structure configuration. The N9083A multi-standard radio measurement application has been enhanced to support non-contiguous test configurations as defined in 3GPP Release 10. This enables one-button measurements of the cumulative adjacent-channel leakage ratio.

Depending on maximum frequency coverage, base pricing ranges from $31,525 to $50,767 for the N9020A MXA and from $17,470 to $36,645 for the N9010A EXA. Fast sweep is included at no extra charge with the purchase of an MXA or EXA configured with select options, or as an upgrade for existing instruments.

Agilent, www.agilent.com/find/X-series_enhancements
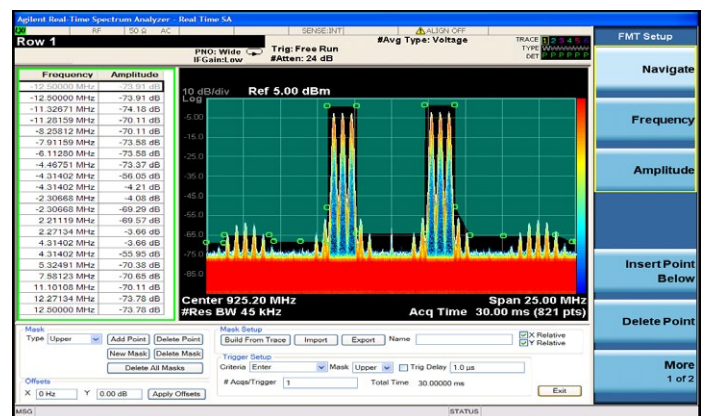
Real-time spectrum analysis displays reflect improved phase-noise performance.

pulse

Simultaneous multi-channel UHF data reception in automotive transceivers

Technology introduced by NXP is claimed to deliver improved RF performance to bring a new dimension to 2-way applications, with significant reduction in overall power consumption. NXP has introduced the NCK2983, a low-power multi-channel two-way UHF transceiver with an embedded microcontroller system that can for the first time receive up to three channels in parallel rather than sequentially. The device is suitable for use in both key fob and body control module-type applications, including keyless entry, remote start, tyre pressure monitoring systems (TPMS) and wireless diagnostics (WD). Existing multi-channel transceivers are only able to poll for signals sequentially, in order to check every possible frequency that an application may be transmitting on. By enabling reception across three channels simultaneously, the NCK2983 device shortens the period it needs to be 'awake' when polling, significantly reducing overall power consumption while increasing system robustness.

Simultaneous UHF data reception improves systems response and cuts battery power in automotive applications.

The NCK2983 is able to receive multiple channels in parallel because it uses a Wideband Digital IF approach. Similar in concept to a Software Defined Radio, the high-performance, low-noise front end presents the down-mixed RF signal to a high-speed sigma-delta ADC, serving as input to up to three discrete receive channels in the DSP unit. Each channel can be configured independently, mixing down the signal to baseband according to the specific channel frequency, and applying relevant channel filter, demodulation and clock recovery settings. The NCK2983 features a fractional–N based frequency synthesiser that enables the device to operate in any of the common ISM bands and supports carrier frequency hopping at each of the three baseband channels. The NCK2983 also includes an embedded microcontroller system with 32 kB EROM (Flash) allowing complete applications to be implemented as single-chip

solutions. The transceiver supports special power modes for battery-powered key and car operation such as sleep mode and low power polling mode. NCK2983 combines RF performance with sophisticated baseband signal processing - suiting the chip to two-way multi-channel applications in the automotive market.

"The NCK2983 is the first chip of a new product family for sub-GHz RF communication systems," said Dr. Volker Graeger, vice president Car Access and Immobilizers, NXP Semiconductors. "... we provide new ways of reducing power consumption while improving performance. By combining multi-channel and simultaneous RF reception with customer-programmable smart polling in a single package, NXP has made another breakthrough in automotive electronics. Next we intend to significantly increase the system operating range by launching a dedicated long-range version of the chip."

Features include; a single IC covers 315, 434, 447, 868, 915 and 950 MHz bands for worldwide usage; simultaneous reception of up to three channels in parallel (within 1.8 MHz IF); 13 channel filter bandwidth options (10 - 600 kHz); operation up to 200 kchips/sec (FSK/ASK); sensitivity of -123 dBm FSK/ASK with high dynamic RSSI measurement; receiver path with two multiplexed antenna inputs enables dual band antenna matching; integrated RX/TX switch (SP2T) for flexible application matching; and power management modes for polling and wake up triggered applications. Its PA has digital controlled power ramping and +12 dBm output power, and there is an integrated 16-bit RISC MCU, plus a co-processor for bit manipulation and cyclic redundancy code calculation (CRC). You control the device over SPI, UART, or LIN and the chip also has a 10 bit ADC sensor interface with up to 100 ksamples/sec sampling rate.

NXP Semiconductors; www.nxp.com/pip/NCK2983AHN

Integrated power solution combines quad buck regulators and 200 mA LDO

A 5-channel power control device from Analog Devices, ADP5052, combines four high performance buck regulators and one 200 mA low dropout (LDO) regulator in a 48-lead LFCSP package that meets demanding performance and board space requirements. The device enables direct connection to high input voltages up to 15V with no preregulators. Channel 1 and Channel 2 integrate high-side power MOSFETs and low-side MOSFET drivers. External NFETs can be used in low-side power devices to achieve an efficient solution and deliver a programmable output current of 1.2A, 2.5A, or 4A. Combining Channel 1 and Channel 2 in a parallel configuration can provide a single output with up to 8A of current. Channel 3 and Channel 4 integrate both high-side and low-side MOSFETs

to deliver output current of 1.2A.

The switching frequency of the ADP5052 can be programmed or synchronised to an external clock. The ADP5052 contains a precision enable pin on each channel for power-up sequencing or adjustable UVLO threshold. It integrates a general-purpose LDO regulator with low quiescent current and low dropout voltage that provides up to 200 mA of output current.

You might use the device, Analog suggests, in small-cell base stations, FPGA and processor applications, security and surveillance, or in medical applications. Features include input voltage range of 4.5 to 15V; ±1.5% output accuracy over full temperature range; 250 kHz to 1.4 MHz adjustable switching frequency; and adjustable/fixed output options via factory fuse.

Analog Devices; www.analog.com/en/power-management/ multi-output-regulators/adp5052/products/product.html

Programmable USB-port power controllers support 12-W fast charging

Microchip has expanded its programmable USB port power controller range with the three-member UC-S100X family. The new power controllers offer advanced USB-based charging capabilities for host devices, such as laptops, tablets, monitors, docking stations and printers, as well as dedicated AC-DC power-supply and charging products, such as wall adapters.

The UCS1001-3, UCS1001-4 and UCS1002-2 are an expansion of Microchip's UCS1001 and UCS1002 series, offering higher current and priority charging. The UCS100X variants have also added support for active cables, such as the Apple Lightning connector, along with 12W charging. The UCS1002-2 features a built-in current sensor that can report on the amount of charging current. This allows a system to optimise its charging current and appropriately allocate power. The UCS100X can support future USB product designs via a flexible method for detecting and creating charging emulation profiles. This allows designers to update their systems as new products are introduced to the market, while providing compatibility with a wider range of existing products.

Charge with up to 12W power from these USB host controllers.

The UCS1001-3, UCS1001-4 and UCS1002-2 come in a 20-pin QFN package, for $0.90 each (5,000). Design support is with the UCS1001-3/4 Evaluation Board (ADM00540, $24.99) and UCS1002-2 Evaluation Board (ADM00497, $90.00)

Microchip; www.microchip.com/get/TKTE

Ultra low power capacitive touch sensing buttons for front panels

Cypress has expanded its CapSense Express mechanical button replacement family with a controller featuring support from its EZ-Click Customiser Tool and embedding its SmartSense Auto-Tuning. This capacitive touch-sensing controller is optimised to replace mechanical buttons in front panels for industrial and consumer applications, portable medical devices, gaming devices and home automation systems.

The low-power CY8CMBR2110 device supports up to 10 buttons and drives up to 10 LEDs with fully configurable LED effects.

The EZ-Click customiser tool is GUI-based software that combines device configuration, visual feedback, and production line testing for register configuration of the CY8CMBR2110 controllers, for faster development. You can use the tool to implement customised LED effects and buzzer output for audio feedback. Controllers in the Mechanical Button Replacement (MBR) family use Cypress's SmartSense auto-tuning algorithm, which eliminates the requirement for manual system tuning and that maintains optimal button performance during run-time.

"The market for front panel user interfaces in industrial, medical and consumer applications is huge and growing," said Dirk Franklin, business unit director for Cypress's CapSense solutions. "Designing a capacitive touch sensing user interface is not easy, but with our CapSense Express MBR family, backed by the support of our customiser tool and auto-tuning technology, Cypress has delivered ease of design for sleek, reliable capacitive touch control panels. What we like to say about our new, button-replacement family is that 'it just works!'"

The CapSense Express MBR family includes the CY8C-MBR2016 matrix keypad unit, the CY8CMBR2010 ten-button

Assisted design steps accelerate the process of replacing buttons with capacitive front-panel sensing.

controllers and the CY8CMBR2044 four-button hardware configurable controllers. Devices in the family offer supply current in run mode of 15 µA per button and a 100 nA Deep-Sleep mode. The devices operate over a 1.71V to 5.5V range, making them suitable for a wide range of regulated and unregulated battery applications, and enabling them to operate from a single coin cell battery. The family delivers robust sensing in noisy environments using Cypress's CapSense Sigma Delta (CSD) sensing method, ensuring immunity to conducted and radiated noise. These devices also feature an integrated voltage regulator to address power supply noise, as well as filters for any spurious noise.

The MBR family's SmartSense auto-tuning dynamically optimises the capacitive baseline and detection threshold for each button. The algorithm adjusts for the optimal capacitance sensing range at power-up and during runtime as environmental conditions change, including noise, temperature, and humidity. Eliminating the need to tune is a significant advantage for large and small manufacturers alike, as it saves engineering time and yield loss that can occur with even slight variations in manufacturing tolerances. This savings is greatly multiplied for customers with a global factory footprint and multi-sourced supply chain. SmartSense auto-tuning can eliminate the need for additional test steps required by competing solutions to address manufacturing variations in PCBs and overlays.

Cypress offers the CY3280-MBR2 CapSense Express with SmartSense Auto-Tuning Evaluation Kit to support the CY8C-MBR2110 controller. The MBR family's accompanying Design Toolbox is an interactive spreadsheet that provides detailed resources to ensure optimal performance and validate CapSense systems. The toolbox delivers system debug features and offers application specific guidelines for capacitive buttons, allowing customers to take designs directly to production.

Cypress; www.cypress.com/go/capsense

MAHMOUD HARMOUCH & TOBIAS NASS, TEXAS INSTRUMENTS

SWITCHER PEAK CURRENT-MODE CONTROL CIRCUIT OPTIMISATION FOR AUTOMOTIVE APPLICATIONS

Switching above 1.7 MHz to avoid AM band interference, and fast load transient response, are now constant pressures in switch-mode power supplies used in automotive infotainment systems. Today's multicore processors and system-on-a-chip (SOC) require core voltages, even below 1V, to be tightly regulated from an intermediate voltage of 2.5V to 6V. At the same time, power supply designers target high-switching frequencies, compact solutions and fast transient responses.

This article studies design optimisation in depth for peak current-mode control loops. This step-by-step design considers parametric variation, parasitic elements, as well as typical automotive requirements. A family of synchronous buck converter devices is used to demonstrate optimisation.

Today's multicore processors and system-on-a-chip (SOC) require low, but tightly regulated core voltage supplies that react very quickly to transients. The following test case depicts an system that requires a core voltage of 1.2V with overall accuracy of ±3%, which includes the transient response. The load transient is specified as 0.5A to 2A within 400 nsec. Additionally, the behaviour during load transients is explained, relevant formulas are derived and applied to the example.

CIRCUIT BEHAVIOUR DURING A LOAD TRANSIENT

During a load transient, the feedback loop takes finite time responding to the current demand. This causes a dip in the output voltage (Figure 1). The duration of this dip is known as the system response time, Tr. During this time the load current is the sum of both inductor and output capacitor currents. The output voltage dip cannot be avoided, but can be minimised to meet the specification.

All calculations provided assume the following definition:
- Io: load current
- Ic: current from output capacitor C_{OUT}
- IL: current from the inductor L
- Tr: loop response time
- V_{OUT}: output voltage

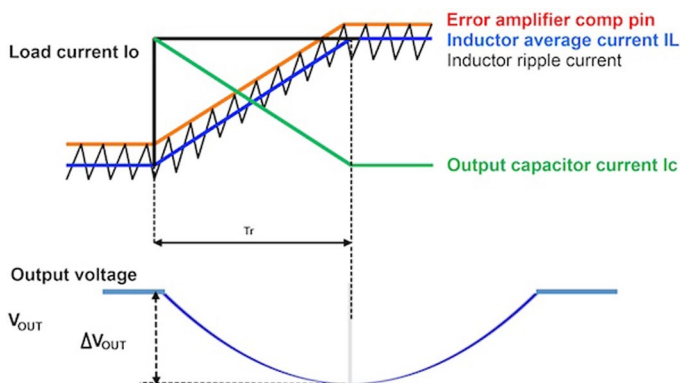**Figure 1:** *Load transient response*

Assuming the load step happens at time zero t = 0, and the parameters initial value are Io(0) = Io, IL(0) = 0, Ic(0) = Io and V_{OUT} (0) = V0, this behaviour can be explained using equations 1 – 3:

$$I_O = I_L + I_C \qquad (1)$$
$$I_L = I_o \cdot \frac{t}{Tr} \qquad (2)$$
$$I_C = -C_{OUT} \cdot \frac{dVout}{dt} \qquad (3)$$

Equation 1 – 3 result in:

$$I_O = I_O \cdot \frac{t}{Tr} - C_{OUT} \cdot \frac{dV_{OUT}}{dt},$$

which can be converted to equation 4:

$$C_{OUT} \cdot \frac{dVout}{dt} = I_O \frac{t}{T_r} - I_O \qquad (4)$$

With an inductor current and the output voltage being continuous functions at t = 0, integrating equation 4 results in equation 5:

$$V_{OUT} = \frac{1}{2} \cdot \frac{Io}{Cout} \frac{t^2}{Tr} - \frac{Io}{C_{OUT}} t + constant \qquad (5)$$

The constant represents the output voltage V0 at t = 0 as

$$V_{OUT} = \frac{1}{2} \frac{Io}{C_{OUT}} \frac{t^2}{Tr} - \frac{Io}{C_{OUT}} t + V_0.$$

The voltage dip during the load step is $\Delta V_{OUT} = V_{OUT} - V0$ (equation 6):

$$\Delta V_{OUT} = \frac{1}{2} \frac{Io}{Cout} \frac{t^2}{Tr} - \frac{Io}{C_{OUT}} t \qquad (6)$$

Equation 6 is a parabolic function and its minimum is when the derivative   This gives the ΔV_{OUT} minimum at t = Tr, or equation 7:

$$\Delta V_{out,min} = \frac{1}{2} T_r \frac{Io}{Cout} - T_r \frac{Io}{Cout} = -\frac{1}{2} T_r \frac{Io}{Cout} \qquad (7)$$

Equation 7 gives the difference between the lowest output voltage during load step and the initial voltage before the load step. The negative sign indicates that the output voltage drops below its initial level. The output voltage dip is proportional to the load step current, feedback loop response time, and is inversely proportional to the output capacitor value.

OPTIMISING TRANSIENT RESPONSE

The design goal is to minimise the output voltage dip of ΔV_{OUT} min. This can be achieved by increasing the output capacitor and lowering the loop response time, Tr, which is a function of the crossover frequency, Fc, given in equation 8:

$$T_r = \frac{0.35}{Fc} \qquad (8)$$

Equations 7 and 8 can be derived to (equation 9):

$$\Delta V_{out,min} = -\frac{1}{2} \frac{Io}{Cout} \frac{0.35}{Fc} \qquad (9)$$

Two important parameters to be optimised are: 1) output capacitor, C_{OUT}, and; 2) crossover frequency, Fc. By increas-

ing these two values, the output voltage dip can be minimised. However, because there is no ideal circuit, the output voltage dip can be minimised only to a certain level. An often limiting factor is the bandwidth of the error amplifier.

OVERALL LOOP TRANSFER FUNCTION

Following basic signal theory, the transfer function $H(s) = V_{out}/Vr$, where Vo is the small signal output voltage and Vr is the return signal.

$$H(s) = \text{power stage gain} \times \text{voltage divider gain} \times \text{output stage gain} \times \text{error amplifier gain} \quad (10)$$

$$\text{Voltage divider gain} \quad \frac{V_{ref}}{V_{out}} = \frac{R2}{R1+R2} \quad (11)$$

$$\text{Power stage gain} = Gm \quad (12)$$

$$\text{Output stage gain} = R_L \frac{1+R_{esr}C_{out}S}{1+(R_{esr}+R_L)C_{out}S} \quad (13)$$

Where RL is the load resistance, ESR is the output capacitor series resistance, and C_{OUT} is the output capacitor (Figure 2):
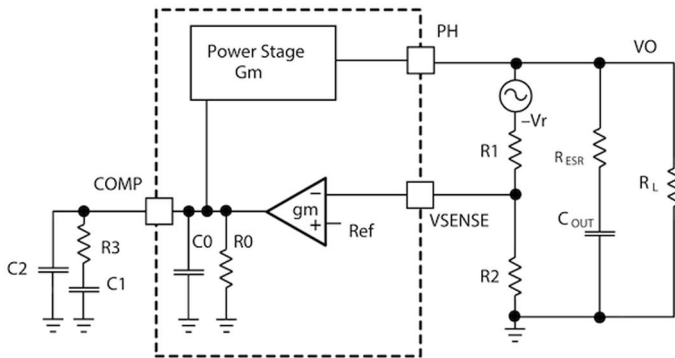

Figure 2: *Small signal model for loop response*

ERROR AMPLIFIER GAIN

The total error amplifier gain depends on the open loop gain and compensation network. For an ideal transcondutance error amplifier, R0 is infinite and C0 is zero. This allows constant gain across an infinite bandwidth. However, a real transconductance error amplifier has a finite output resistance and a small capacitance. These values impact the error amplifier gain. As they often are not specified, they are calculated from the unity gain bandwidth.

The error amplifier is a transconductance amplifier with V_{SENSE} input and V_{COMP} output. The error amplifier output current i is proportional to V_{SENSE} and $i = gm \times V_{SENSE}$.

The error amplifier output voltage, V_{COMP}, is the output current i multiplied by the compensation network impedance Z formed by R3, C1 and C2. Also, the internal impedance, Z0, formed by R0 and C0 need to be taken into consideration (equation 14):

$$Z_0 = \frac{R_0}{1+R_0C_0S} \quad (14)$$

With that, the transconductance amplifier open loop transfer function can be calculated as (equation 15):

$$A(S) = g_m \frac{R_0}{1+R_0C_0S} \quad (15)$$

Equation 17 is a first order transfer function with DC gain of gm·R0 and a pole at 1/(2πR0C0).

The error amplifier can be considered as ideal at low frequencies, but the bandwidth is limited due to this pole. Typical error

amplifier bandwidth ranges from 3 to 5 MHz.

Transforming equation 15 into the frequency domain $S = j2\pi F$, the transconductance amplifier open loop transfer function is defined as (equation 16)

$$A(j2\pi F) = \frac{g_m R_0}{1+j2\pi FR_0C_0} \quad (16)$$

with an amplitude as in equation 17 and phase of $\tan(\emptyset) = -2\pi FR0C0$.

If the error amplifier unity gain bandwidth is specified, R0 and C0 can be calculated as in equation 18 & 19, assuming a unity gain bandwidth of 5 MHz. As 2πFR0C0>1 at UGBW (unity-gain bandwidth), the gain can be simplified to equation 17:

$$|A(j2\pi F)| = \frac{g_m R_0}{\sqrt[2]{1+(2\pi FR_0C_0)^2}} = \frac{g_m R_0}{2\pi FR_0C_0} = 1 \quad (17)$$

Equation 19 can be derived to calculate equation 18:

$$C_0 = \frac{gm}{2\pi F} \quad (18)$$

where gm is the specified transconductance and F is the UGBD.

Applying a calculation example with gm = 250 μA/V and UGBD = 5 MHz, C0 is calculated as C0 = (250μA/V)/2πx5MHz=7.9 pF.

At unity gain bandwidth the phase is very close to –90°. For example, a first approximation is Ø = –89.9° and tan(Ø) = –573. This gives:

$$R0 = \frac{-573}{-2\pi FC0} = \frac{-573}{-2\pi x5MHzx7.9pF} \quad (19)$$

and R0 = 2.3 MΩ. The very high output impedance will be neglected later on and, therefore, justifies the first order approximation.

COMPENSATION IMPEDANCE Z

Another factor of the error amplifier gain is the compensation network impedance that can be calculated as:

$$Z = \left(R_3 + \frac{1}{C_1S}\right) \| \frac{1}{C_2S} = \frac{\frac{1+R3C1S}{C1S} \cdot \frac{1}{C2S}}{\frac{1+R3C1S}{C1S} + \frac{1}{C2S}} \quad (20)$$

which can be resolved to equation 21:

$$Z = \frac{1+R_3C_1S}{(C_1+C_2)S(1+R_3\frac{C_1C_2}{C_1+C_2}S)} \quad (21)$$

The total error amplifier output impedance is the equivalent impedance of

$$Z_0\|Z = \frac{\frac{R_0}{1+R_0C_0S} \times \frac{1+R_3C_1S}{(C_1+C_2)S(1+R_3\frac{C_1C_2}{C_1+C_2}S)}}{\frac{R_0}{1+R_0C_0S} + \frac{1+R_3C_1S}{(C_1+C_2)S(1+R_3\frac{C_1C_2}{C_1+C_2}S)}} \quad (22)$$

which can be calculated as (equation 23):

$$Z_0\|Z = R_0 \frac{1+R3C1S}{1+(R0C1)S+R0R3C1(C0+C2)S^2} \quad (24)$$

The denominator of equation 21 is a second degree equation and can be factorised by making the right approximation. The compensation resistor, R3, is in the order of a few-10-kΩ, so

R3 << R0. The compensation capacitor, C1, is in the order of a few nF, and the high-frequency decoupling capacitor, C2, is in the order of a few-10-pF, so C0 + C2 << C1. This approximation leads to equation 24:

The denominator discriminant = $(R0.C1)^2 - 4R0.R3.C1(C0 + C2) = R0.C1(R0.C1 - 4R3(C0 + C2))$. Using the same approximation R0C1 >> 4R3(C0 + C2). The simplified discriminant is $(R0.C1)^2$.

This results in the roots S1 = 0 and $-\frac{1}{R3(C0+C2)}$, and a total

approximated error amplifier output impedance of $\frac{1+R3C1S}{C1S(1+R3(C0+C2)S)}$.

With that, all factors of the transfer function are described and the overall open loop transfer function given in equation 10 can be calculated as equation 25:

$$H(s) = \underbrace{G_m}_{\text{Power Stage Gain}} \underbrace{\frac{R_2}{R_1+R_2}}_{\text{Voltage divider gain}} \underbrace{R_L \frac{1+R_{esr}C_{out}S}{1+(R_{esr}+R_L)C_{out}S}}_{\text{Output Stage Gain}} \underbrace{\frac{g_m}{C_1S} \frac{1+R_3C_1S}{1+R_3(C_0+C_2)S}}_{\text{Error Amplifier Gain}} \quad (25)$$

CALCULATING COMPENSATION VALUES

After deriving the open loop transfer function, the right components for achieving the desired bandwidth and phase margin have to be calculated.

The error amplifier and power stage transconductances, Gm and gm, are specified in the device datasheet. The output capacitor, C_{OUT}, and inductor are calculated for achieving low-output ripple voltage at the switching frequency. Transforming equation 25 into the frequency domain and entering equation 13, the transfer function can be calculated as equation 26:

$$H(j\omega) = R_L G_m \frac{V_{ref}}{V_{OUT}} \frac{1+jR_{esr}C_{OUT}\omega}{1+j(R_{esr}+R_L)C_{OUT}\omega} \cdot \frac{g_m}{jC_1\omega} \cdot \frac{1+jR_3C_1\omega}{1+jR_3(C_0+C_2)\omega} \quad (26)$$

From this transfer function, we can clearly identify the DC

gain as $R_L G_m \frac{V_{ref}}{V_{out}}$. It also shows two dominant poles,

$\frac{1}{2\pi(R_{esr}+R_L)C_{OUT}}$ & $\frac{g_m}{2\pi C_1}$, and one dominant zero at $\frac{1}{2\pi R_3 C_1}$.

To simplify the calculation, the following assumptions are made. The output capacitor is a low ESR ceramic of less than 5 mΩ and, therefore, is zero at a higher frequency. C2 is too small to decouple a high frequency, and also can be neglected. For an easier calculation of the crossover frequency Fc and phase margin ΔØ, the gain is simplified as equation 27:

$$H(j\omega) = R_L G_m \frac{V_{ref}}{V_{out}} \frac{1+jR3C1\omega}{1+jRLCout\omega} \frac{gm}{jC1\omega} \quad (27)$$

The result is a gain of $|H(j\omega)| = R_L G_m \frac{V_{ref}}{V_{out}} \frac{\sqrt{1+(R3C1\omega)^2}}{\sqrt{1+(RLCout\omega)^2}} \frac{gm}{C1\omega}$. As the

design goal is to achieve high crossover frequency, it can be assumed that $1<(R_3.C_1\omega)^2$ and $1<(R_L C_{out}\omega)^2$. With this approximation the gain can be simplified to equation 28:

$$|H(j\omega)| = R_L G_m \frac{V_{ref}}{V_{out}} \frac{R3C1\omega}{RLCout\omega} \frac{gm}{C1\omega} \quad (28)$$

At the crossover frequency H is equal to 1, which leads to

$G_m \frac{V_{ref}}{V_{out}} \frac{R3}{Cout} \frac{gm}{2\pi Fc} = 1$, which can be converted to equation 29:

$$R_3 = \frac{V_{out}}{V_{ref}} \frac{Cout}{gm} \frac{2\pi Fc}{Gm} \quad (29)$$

Calculating the phase of equation 25 results in equation 30:

$$\emptyset = -90° - atan(R_L C_{out}\omega) + atan(R_3 C_1\omega) \quad (30)$$

For a stable design, the phase margin is targeted at > 45°. However, for a robust design, and taking the additional phase drop due to slope compensation into account, the compensation is set to reach Ø = -90° at the crossover frequency.

This is the case if atan($RLC_{out}\omega$) is equal to atan($R_3C_1\omega$), which results to equation 31:

$$C_1 = \frac{R_L C_{out}}{R_3} \quad (31)$$

At higher frequencies, the output capacitor ESR creates a zero and results in increasing gain, which can introduce high-frequency noise. To compensate, a pole created by C2 can be used and should be set to near the ESR zero. In this case, C2 is set to equation 32:

$$C_2 = \frac{R_{esr} C_{out}}{R_3} \quad (32)$$

CROSSOVER FREQUENCY

The next step is to place the target crossover frequency. At lower frequencies the output stage is a voltage-controlled current source. The power stage gain Gm is constant at low frequencies. However, at higher frequency between one-sixth and two-thirds of the switching frequency, Gm has a pole of –20 db/decade and a phase at –90º. Therefore, the crossover frequency is limited. (The basic principle of current-mode control is explained in references 1, 2 and 3.) To account for this limitation, it is better to be conservative and choose the crossover frequency at one decade below half the switching frequency. With a 2 MHz switching frequency, the crossover is set to 100 kHz.

CALCULATION EXAMPLE

Following the theoretical description of the behaviour above, the derived formulae are applied to an example. In our example we used TI's TPS57114, an automotive catalogue 2.95V- to 6V-input, 4A, 2 MHz synchronous step down SWIFT DC/DC converter [4].

The design targets for this example are to meet typical requirements for an automotive infotainment SoC.

Parameter	Design Target
V_{IN}	5V
V_{OUT}	1.2V
Switching frequency F	2 MHz (above AM band, 1.7 MHz)
Ouput voltage ripple	<5 mV
Inductor ripple current	<1A P-P
Max. load current $I_{OUT,MAX}$	4A
Load transient	0.5–2A, 500 ns slew rate
Load transient response	+/–2.5%
Error amplifier transconductance gm	245 µA/V
Power stage transconductance Gm	25 A/V
Vref	0.8V
Crossover frequency	100 kHz

Table 1: *Design Targets*

SELECTING SWITCHING FREQUENCY

To ensure that the switching frequency is well above the AM band while allowing high bandwidth and small components, 2 MHz is selected.

OUTPUT CAPACITOR CALCULATION

The output voltage ripple during steady state is caused by the ESR of the output capacitors, as well as the output capacitor size itself (equation 33).

$$V_{out,pp} = \Delta I_L \left(R_{ESR} + \frac{1}{8 C_{out} F} \right) \qquad (33)$$

To optimise the ripple performance and transient response, use a low series resistor (ESR) ceramic capacitor. Nevertheless, a realistic ESR of 2 mΩ results in 2 mV ripple. and the resulting ripple contribution of the $_{out}$put cap is only 3 mV. With a switching frequency of 2 MHz, C_{OUT} can be calculated as equation 34:

$$C_{out} = \frac{\Delta IL}{V_{out,pp}\ 8F} = \frac{1A}{3mV \cdot 8 \cdot 2MHz} = 20.8 \mu F \qquad (34)$$

Beside the output voltage ripple, the transient response is another variable determining the output capacitor size. Applying formula 9 to this example, we get

$$C_{out} = \frac{1}{2} \frac{Io}{\Delta V_{out,min}} \frac{0.35}{Fc} = \frac{1}{2} \frac{1.5A}{30mV} \frac{0.35}{100kHz} = 87.5 \mu F \qquad (35)$$

To select the right output capacitor size, the larger numbers of equation 34 and equation 35 should be selected. In order to add some margin 5 x 22 µF are selected.

CALCULATING THE COMPENSATION NETWORK

Using equation 29, the compensation resistor, R3, can be calculated as $R_3 = \frac{Vout\ Cout}{Vref\ gm} \frac{2\pi Fc}{Gm} = \frac{1.2}{0.8} \frac{110\mu F}{245\frac{uA}{V}} \frac{2\pi 100kHz}{25\frac{A}{V}} = 16.9 k\Omega.$

A standard value of 18 kΩ is selected. Equation 31 then leads to $C_1 = \frac{\frac{Vout}{Iout,max} Cout}{R_3} = \frac{\frac{1.2V}{4} 110\mu F}{18k\Omega} = 1.83 nF$ and a standard value of 1.8 nF is used.

Finally, the capacitor, C2, is calculated as

$C_2 = \frac{R_{esr}C_{out}}{R_3} = \frac{2m\Omega\ 110\mu F}{18k\Omega} = 12.2 pF.$ The selected standard value is

10 pF. With these numbers, also used on the existing evaluation module, the frequency response can be measured. The crossover frequency is 80 kHz with a phase margin of ~45 degree.
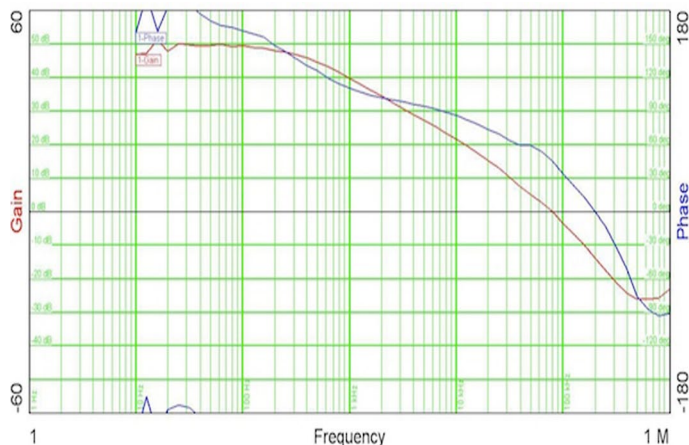With this crossover frequency, the resulting transient re-

Figure 3: *Measured frequency response*

sponse can be calculated, using equation 7:

$$\Delta V_{out,min} = \frac{1}{2}\frac{1.5A}{110uF}\frac{0.35}{80KHz} = 29.8mV$$

Applying a transient response to the circuit results into a
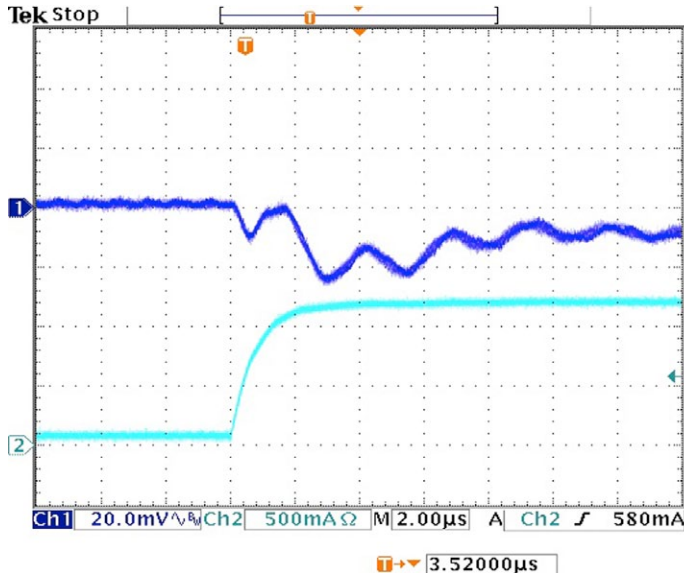
--transient response of ~30 mV (Figure 4).

CONCLUSION

Load transient response is a critical parameter for power supplies: in order to optimise this parameter, this article has looked at a theoretical explanation of the circuit's behaviour. After applying an example to the derived formulas, the resulting circuit has been built and characterised. The measured transient response and crossover frequency proves the step-by-step approach developed here.

REFERENCES

1 . "Venable Technical Paper#5, Current-Mode Control," Venable Industries, http://dc195.4shared.com/doc/0soglPxp/preview.html

2 . Lloyd H. Dixon, Jr., "Current mode control of switching power supplies," Texas instruments, 2001, http://www.ti.com/lit/an/slua079/slua079.pdf

3 . "Hiroki SAKURAI, Yasuhiro SUGIMOTO, "Analysis and Design of aCurrent-Mode PWM Buck Converter Adopting the Output-Voltage IndependentSecond-Order Slope Compensation Scheme," IEICE Trans. Fundamentals, Vol. E88-A, NO. 2, February 2005, http://www.elect.chuo-u.ac.jp/sugimoto/publications/pdf/2007/saku4.pdf

4 . "2.95 V to 6 V Input, 4-A Output, 2MHz, Synchronous Step Down Switcher (Rev. B),"

LED-driving techniques reduce power in LCD TVs

New design techniques in LED-driver circuits promise to deliver significant energy savings.

Peter Rust, Werner Schögler, Manfred Pauritsch, and Herbert Truppe • AMS AG

According to the SEAD (Super-efficient Equipment and Appliance Deployment) initiative, televisions are responsible for approximately 3% to 8% of global residential electricity consumption. An analysis conducted by Lawrence Berkeley National Laboratory suggests that advances such as more efficient LED driving can yield major reductions in television electricity consumption in the coming years. There seems little doubt that liquid-crystal-display (LCD) technology with LED backlighting is the only viable way to reach the efficiency targets that authorities are proposing. Plasma has the disadvantage that each pixel is an active light emitter, so power consumption is directly proportional to the number of pixels. As a result, high-definition plasma televisions consume approximately two to three times the power of an LCD TV for the same resolution and brightness.

LED-driving techniques reduce power in LCD TVs

Highly touted organic light-emitting-diode (OLED) technology, as recently reported, may not come anytime soon, if ever. The investment required for this "bleeding edge" large-panel technology is prohibitive. In contrast, large display panels with state-of-the-art thin-film-transistor LCD technology and "smart" direct LED backlighting with local dimming are far less expensive than OLEDs but compare well for both power consumption and picture quality.

Today's LCD TVs—even those with LED backlighting—are still some distance from achieving the efficiency targets they will face in the coming years. New design techniques in LED-driver circuits, however, promise to deliver significant energy savings that will go a long way toward helping TV manufacturers meet tough requirements for power consumption.

CHANGING REQUIREMENTS
Standards for TV power consumption were raised in 2008, and each year the specification reduces the amount of power a TV can draw. The current maximum for any size screen is 85W, making the design challenge even tougher for large-screen TVs.

Energy Star is an international standard for energy-efficient consumer

AT A GLANCE

⬈ Standards regulating TV power consumption continue to strengthen, meaning designers must develop new ways to meet efficiency targets.

⬈ LED backlighting accounts for 30% to 70% of overall system power in LCD TVs, making this area a good candidate for improving energy efficiency.

⬈ Manufacturers are investigating sophisticated methods for reducing power consumption, including feedback regulation and smart dimming.

products. Compliance is voluntary—and highly influential—but it's not the only form of regulation. The state of California's Energy Commission, for example, introduced its own standard, which went into effect in 2011. This regulation is a bit tougher than Energy Star and also has real teeth: It prohibits the sale of TVs in California that do not meet the state's efficiency specifications.

In Europe, regulations have for many years allowed direct comparison of the energy consumption of white goods (EU Energy Label), and customers use it as a basis for purchasing decisions. These regulations are now mandatory for TVs, cars, and household appliances.

LED BACKLIGHTING
LED backlighting power ranges from 30% to 70% of overall system power in LCD TVs, so improvements in the efficiency of the backlighting power circuit can make a considerable contribution to system efficiency. As is often the case in power system design, a number of small improvements in efficiency can deliver a large combined saving.

There are two ways to implement LED backlighting (**Figure 1**). In indirect, or edge-lit, backlighting, the LEDs are arranged at the edges of the screen. A light guide distributes the light uniformly across the display. This arrangement can be deployed with good optical uniformity in screen sizes up to 60 in. and enables backlighting units with a thickness of just 5 to 10 mm.

In direct-backlit systems, the LEDs are located directly behind the LCD, enabling low power, good thermal design, and excellent scalability with practically no limit to the screen size. These panels tend to be thicker than edge-lit versions, but with the latest technologies

Figure 1 *LCD TVs can adopt one of two arrangements for LED backlighting: indirect (edge light) (a) or direct (b).*
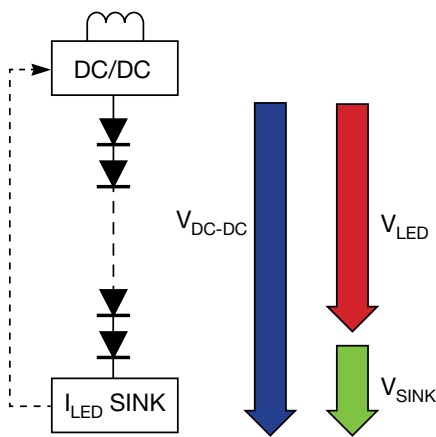
Figure 2 *To minimize power dissipation in a single-string, single-dc/dc-converter backlight system architecture, the voltage at the I_{LED} sink needs to be a fraction above the voltage necessary to guarantee that the LEDs receive their specified current.*

for light distribution, displays as thin as 8 mm can now be found. An important advantage of direct backlighting is that it enables sophisticated local dimming, which lowers power consumption and increases the dynamic contrast ratio, allowing the latest TV designs to compare favorably with OLED technology.

SYSTEM ARCHITECTURE

The choice of architecture for a backlit LED-driver system is the decision with the greatest potential to produce power savings and significantly enhanced picture quality. The designer looks for the best balance between local control of strings of LEDs and the lowest possible BOM.

In a single-string, single-dc/dc-converter backlit system, a switched-mode power supply (SMPS) is used to provide the voltage for backlit LEDs arranged in strings. A current sink is included to regulate the current through the LED string. To minimize power dissipation, the voltage at the I_{LED} sink needs to be a fraction above the voltage necessary to guarantee that the LEDs receive their specified current (**Figure 2**).

A common design approach is to use a feedback path from the I_{LED} sink to the SMPS to regulate the SMPS's output voltage. This feedback path is required to allow for variations in forward voltage (V_F) from one LED to another. The typical forward voltage of a white LED is approximately 3.2V—and may vary as much as ±200 mV per LED—so, for example, in a string of 10 LEDs, the total for V_{LED} may range from 30 to 34V.

The voltage that is required at the dc/dc converter can be expressed as $V_{DC-DC}=V_{LED}+V_{SINK}$; $V_{LED}=nx\ V_{F(LED)}$. V_{SINK} is assumed to be 0.5V, so the I_{LED} sink must regulate V_{DC-DC} in the range of 30.5 to 34.5V, depending on the actual LED forward voltages.

A single string of LEDs is rarely adequate because, as the number of LEDs in the string increases, the required output voltage also increases. Above a certain V_{OUT}/V_{IN} ratio, the SMPS's efficiency falls dramatically. LED-backlight designers can therefore use several strings in order to avoid an excessively high output voltage required of the SMPS.

The simplest approach is to duplicate the single-string, single-dc/dc-converter topology at each string (**Figure 3**). The advantage is efficiency, because each string's voltage is regulated separately. The disadvantage is the high cost, since each string requires its own dc/dc converter, MOSFET, coil, diode, and output capacitor. In order to save on BOM cost, the designer could reduce the number of LED channels, using long strings with many LEDs in each string. This approach, however, compromises the system's ability to implement local dimming, which is another important power-saving technique. Therefore, none of the trade-offs of this topology is particularly attractive.

A more radical approach to reducing BOM cost can be found in the multistring, single-dc/dc-converter topology (**Figure 4**). The drawback of this approach is that the SMPS voltage must be regulated higher than the LED string with the highest forward voltage, which means that it operates at a higher voltage than is necessary for those strings with a lower forward voltage. As a result, the I_{LED} sink must dissipate the excess power from the strings with lower forward voltage, generating heat that must be conducted away from the circuit board and resulting in reduced power efficiency.

The architecture that provides the best balance between efficiency and BOM cost is one that combines elements of the multistring and multi-dc/dc-converter architectures described previously. This mixed architecture (**Figure 5**) has multiple dc/dc converters supplying groups of LED strings.

The multistring, mixed-architecture solution offers the best overall power efficiency because it combines the advantage of local dimming in direct-backlit systems with good dc/dc

output voltage regulation. It also offers a substantial BOM saving over the efficient multistring, multi-dc/dc-converter architecture.

REGULATING CURRENT

The LED-manufacturing process causes wide variations in brightness and color temperature from one LED to the next. As a guide to users, white-LED manufacturers allocate each manufactured unit to groups, or "bins," of LEDs with comparable performance in terms of color, brightness, and forward voltage. But the manufacturer's specification for each brightness and color-temperature bin is valid only under specific nominal operating conditions. This means that the LED current must be set to the nominal current stated in the data sheet in order to generate the specified brightness and color.

Consequently, dimming and brightness control can be implemented only by switching the current sent to any single LED to either on (nominal current) or off (zero current) through a digital PWM control signal. In analog dimming, the LED would be operating outside its specified nominal current, leading to unacceptable changes in color temperature and poor LED-to-LED brightness matching (**Figure 6**).

CURRENT-SINK PROPERTIES

Since LEDs require a perfectly regulated constant-current power supply, it follows that the primary role of the LED driver is to set the current to the nominal value when on and to 0A when off. Therefore, the feedback loop controlling the accuracy of regulation requires an extremely precise current sink (**Figure 7**).

While there are a variety of current-sink designs, the precision requirements of TV backlighting (current regulation better than ±-0.5%) require an accurate op amp to set the I_{LED} current independent of the I_{LED} voltage. In backlighting driver applications, however, the task is more challenging because the accuracy of current regulation must be maintained even when the voltage at the current sink falls to very low levels.

This requirement is difficult to meet, but four generations of accurate current-sink LED drivers from AMS have been designed specifically for such applications. The AS369x, AS381x, AS382x, and AS385x devices also incorporate an offset-compensated op amp. Current-sink drivers require a minimum voltage at the drain ($V_{DS(SAT)}$) to ensure the full accuracy and proper operation of the
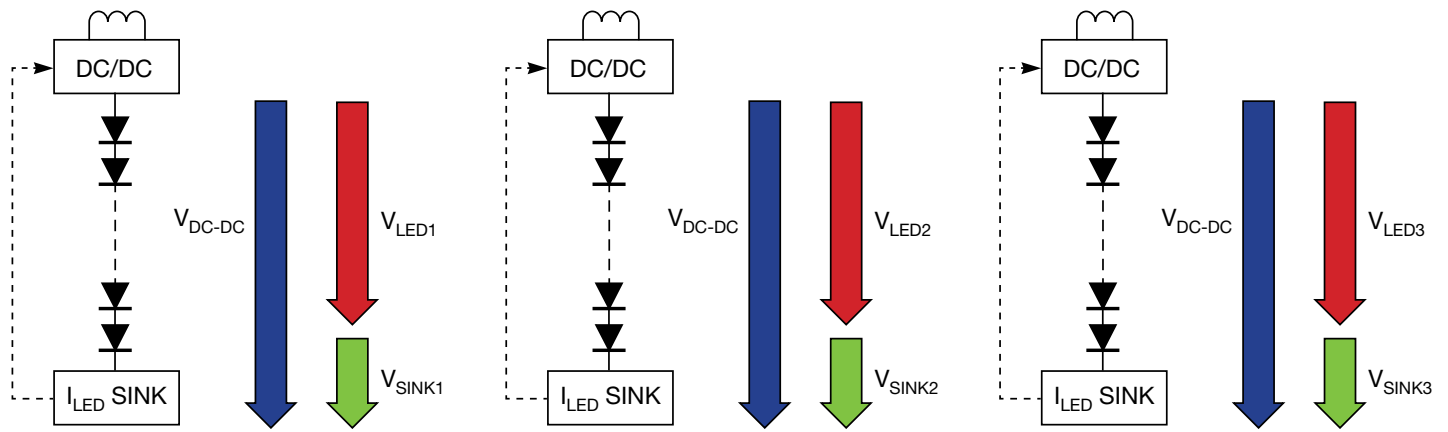
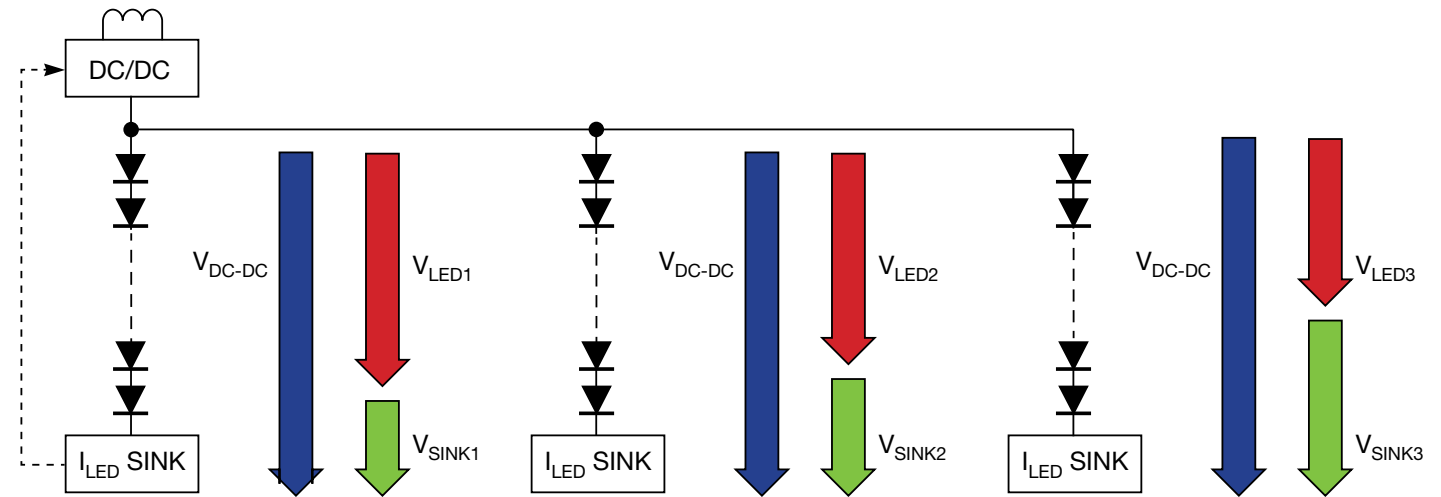Figure 3 *A separate dc/dc converter with each LED string is an expensive option.*

Figure 4 *With one dc/dc converter serving multiple LED strings, SMPS voltage is not optimized.*
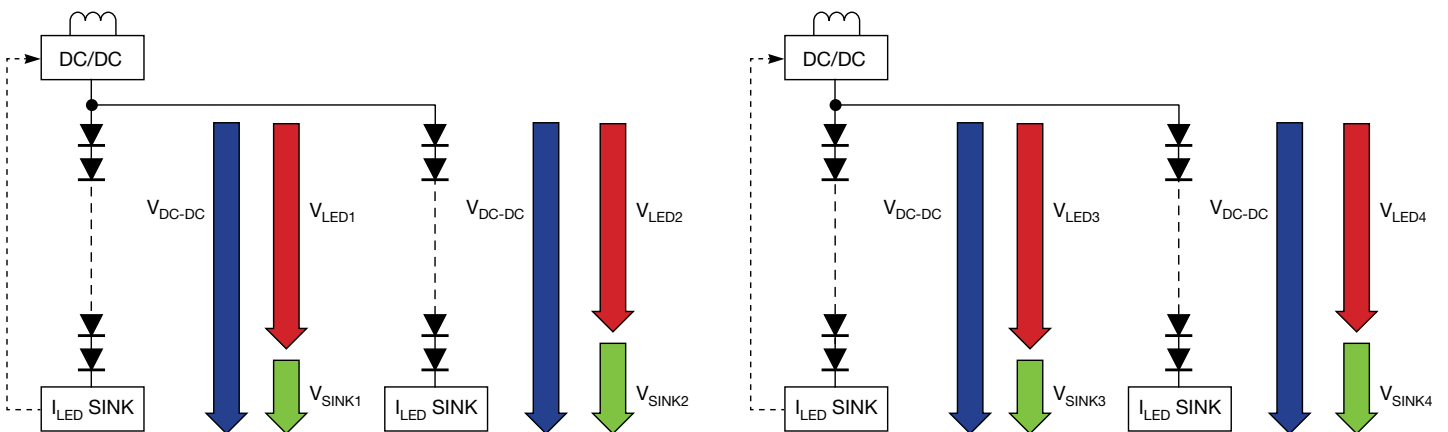

Figure 5 *A mixed architecture optimizes the balance between BOM cost and power efficiency.*

sink transistor inside the saturation region. For the saturated region, the gate-source voltage primarily controls the output current.

If the current sink is to operate at high efficiency, it is important that the voltage drop between V_{SET} and V_{DS} is low. LED drivers with op amps that include built-in offset cancellation can maintain V_{SET} at levels as low as 125 to 250 mV. Allowing an additional margin for V_{DS} above $V_{DS(SAT)}$ of 150 mV, a total voltage drop at the current sink of approximately 400 mV is necessary. For a string of eight LEDs (where V_F=8x3.2=25.6V), this results in a power loss of approximately 1.5% in I_{SINK}. Without the offset cancellation included in the AMS backlight LED drivers, the value of V_{SET} would be higher, leading to higher power losses at the current sink.

POWER OPTIMIZATION

As described earlier, a feedback path from the LED driver to the SMPS sets the drain voltage to the minimum required value. The output current sink can be implemented either with a simple, defined current output driver and an external capacitor (**Figure 8a**) or with a digital control circuit that sets attack/release times and controls the current output with a digital-to-analog converter (I_{DAC}) (**Figure 8b**).

Both of these solutions offer good efficiency, work with every type of SMPS with voltage feedback, and can be implemented by attaching feedback lines from more than one driver to the same SMPS, as is required in mixed-architecture systems. The second, digital implementation, however, provides some special advantages. In addition to not requiring an output capacitor, the digital circuit gives the designer the freedom to define the feedback system's attack and decay times. Combining a fast attack time with decay latency and relatively slow decay can improve the display's performance.

This benefit is particularly noticeable in scenes that require brightness to change rapidly. In this case, a fast attack time eliminates perceptible brightness artifacts as the screen changes from dark to full brightness. The analog solution dims the LEDs' output gradually during a short dark frame, resulting in a visible delay in achieving full brightness for the next bright frame.

This delay is a noticeable distraction for TV viewers because films and other video content create large dynamics from one frame to another. Such artifacts can be eliminated with digital

regulation circuits by inserting latencies of several hundred milliseconds into the decay instruction. Thus, when bright frames are interrupted by a short sequence of dark frames, the second bright frame starts at full brightness because the driver has automatically delayed the voltage ramp-down.

Another useful feature integrated in LED-driver ICs is a fast SPI. In direct-backlit TVs, the LEDs are arranged in a

large number of relatively short strings so that small areas of the panel can be dimmed to save energy. Typically, such arrangements contain 256 channels in a matrix of 16x16 fields, each individually configured through PWM. But generating 256 PWM signals with variable PWM width and delay is a hugely intensive processing task, even for the fastest microcontroller.

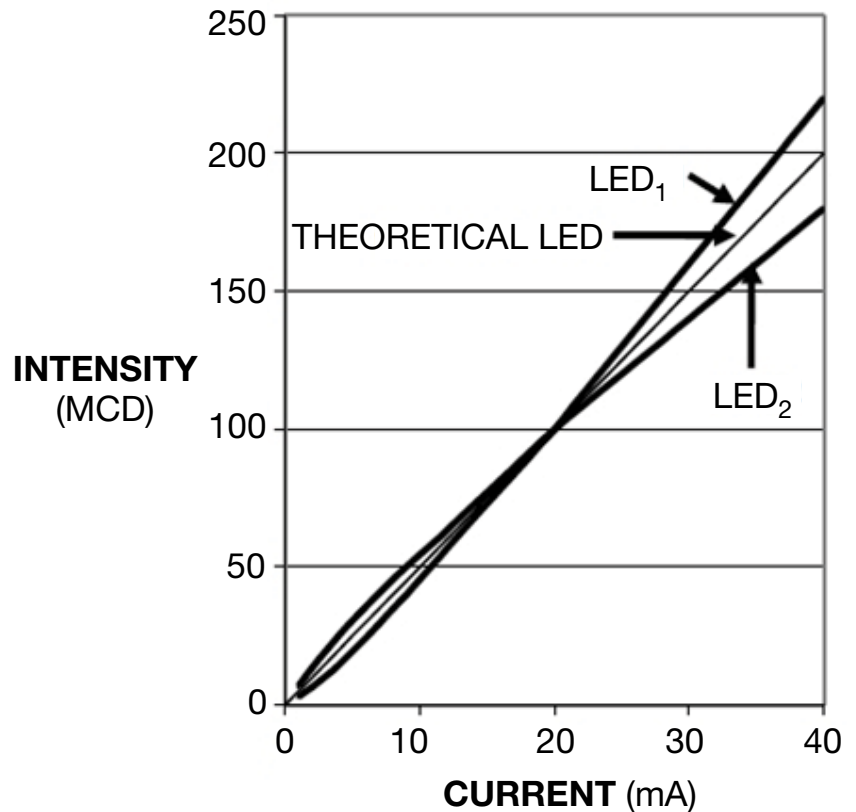These backlighting systems therefore

Figure 6 *The brightness of LEDs from the same bin is guaranteed to match only at nominal current (in this case, 20 mA).*
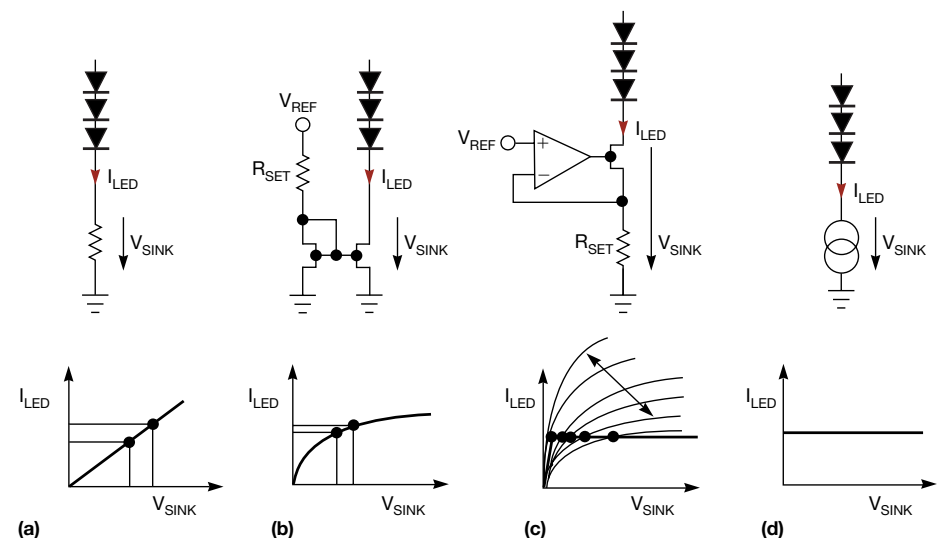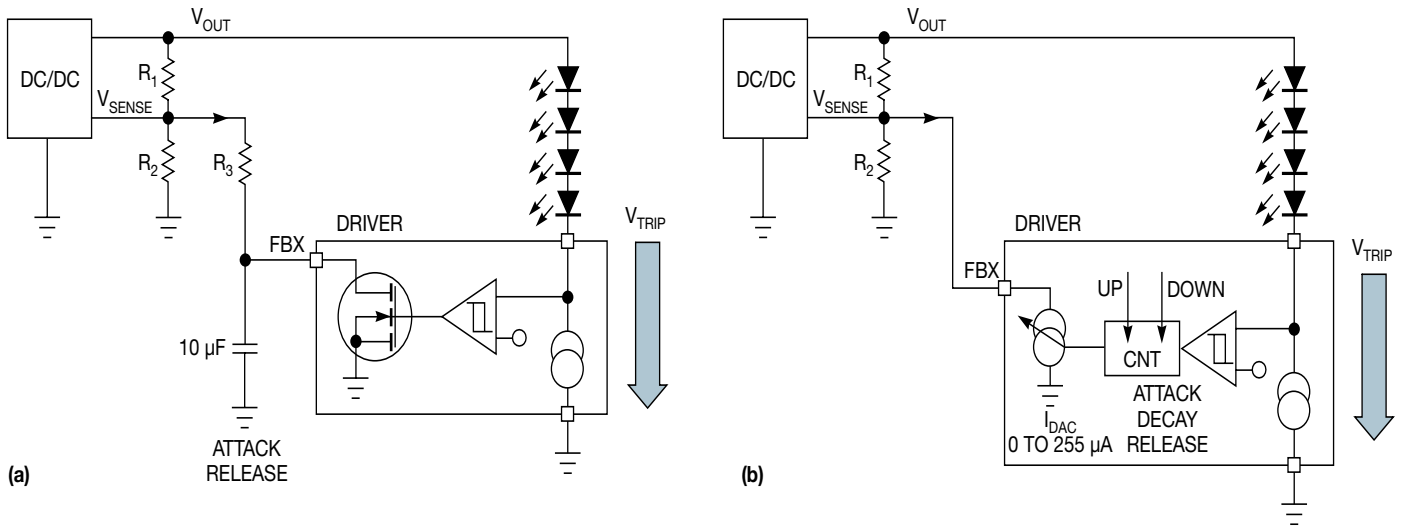

Figure 7 *Of the current-sink designs—primitive (a), simple (b), precision (c), and ideal (d)—a precision current sink requires an accurate op amp with offset compensation.*

LED-driving techniques reduce power in LCD TVs

Figure 8 *Two different methods can be used for applying a feedback loop to the SMPS: The output current sink can be implemented either with a simple, defined current output driver and an external capacitor (a) or with a digital control circuit that sets attack/release times and controls the current output with a DAC (I_{DAC}) (b).*

use local PWM generators integrated into the LED-driver ICs. This approach enables brightness to be configured with simple SPI data transfers. In an architecture with multiple driver ICs (for example, 256 channels with 16 channels per IC and 16 ICs), the LED channels can be configured by daisy-chaining SPI signals and transferring the data that are used in a V_{SYNC} frame to the frame before. In this arrangement, data transfer over an SPI can reach speeds of 20 Mbps, or 50 kb/frame at a 400-Hz frame rate—fast enough to change dimming of each field in sync with the actual frame. Ideal local dimming then can be achieved with minimum overhead on the microcontroller.

SMART DIMMING

This local dimming technique is possible only with direct-backlit systems. But a certain amount of smart dimming also can be achieved with edge lighting. In particular, PWM dimming can be used to vary brightness without changing the color temperature of the white LEDs. Instead of having the edge-lit LEDs permanently set to a specific brightness value, the brightness can be dynamically altered via changes to the pulse width.

Another technique for saving power is dynamic luminance scaling. With this technique, the LCD's white/brightness level is increased in certain scenes to allow the backlight LEDs' power output to be reduced.

Yet another method to reduce power consumption is the use of ambient-light sensors. If the room where the TV is being watched is fairly dark, the backlight brightness can be reduced (**Table 1**).

TV manufacturers are exploring even more sophisticated methods. For instance, cameras are beginning to be designed into displays to enable consumers to use video-telephone services such as Skype on their TVs. These cameras also can be used to detect if someone is actually watching TV; if the TV is on without anyone being in the room, the backlight is reduced to a minimum brightness level.

Even customized energy-consumption patterns can be implemented. While you might prefer watching TV in the energy-friendly eco-mode with reduced backlighting, another member of the household might prefer full brightness.

Considerable power savings can be realized by implementing today's advanced techniques for efficient LED driving. This is important, because ever-tougher regulations continue to reduce the maximum power that a new TV can consume.**EDN**

AUTHORS' BIOGRAPHIES

Peter Rust, Werner Schögler, and Manfred Pauritsch are senior design engineers at AMS.

Herbert Truppe is a product-line manager at AMS.

Table 1 Energy-saving potential using smart LED drivers and smart Ambient-light sensors (ALSs) in LED TVs			
TV LED-backlight architecture	Power-reduction method	Energy-saving percentage LED backlight	Energy-saving percentage LED backlight and ALS
Global dimming	Global dimming with phase shift	5%	25%
Edge local dimming	Edge smart dimming	10% to 20%	40% to 50%
Direct local dimming	Local dimming	20% to 30%	50% to 60%

Agilent
Basic Instruments

Seeing DMM
data in new
ways helps you
work faster

See page 3.

Agilent Technologies

Modern instruments can simplify and accelerate your work

For years, post-measurement analysis usually involved multiple steps of transferring data to a PC and using a variety of software tools to find the insights you needed. However, today's instruments pack an increasing amount of onboard processing power that can change the way you do everything, from routine tasks to corner-case troubleshooting.

The new Agilent 34461A True*volt* DMM is a good case study in how this processing power yields deeper analysis with built-in math functions, more insights in less time with visual feedback, and simplified documentation and distribution of data.

Deeper analysis with built-in math functions

Instruments with analysis capability can deliver deeper insights right from the front panel display.

For instance, the engineers working on a high-power solar charger for smart phones and tablets needed to rigorously test the circuit that detected low solar-cell power for shutting down and restarting the charging circuit smoothly. A 34461A set up to measure the on/off output voltage of the detector circuit displayed the results using the histogram mode, helping the customer troubleshoot and resolve intermittent behavior in a design.

At frequencies below 1 Hz, the display clearly showed a binary distribution, which was the desired result. However, they found that for higher frequencies, which occurred when they waved a hand across the solar panel, the circuit exhibited an anomaly that caused an intermediate output value **(Figure 1)**. This anomaly clearly interfered with the proper output charging operation. A relatively simple design change to the cutoff frequency in the detector circuit solved the problem and eliminated potential customer warranty claims.

More insights in less time with visual feedback

Whether you need occasional confirmation during a running test or interactive feedback during tuning

or troubleshooting, a display that shows you exactly what you need to see can save time and keep you focused on your work.

For example, during some procedures all you want is a quick visual check, and numerical precision can slow you down with unnecessary information. For these scenarios, the bar meter display in the 34461A gives an at-a-glance indication of the measurement value **(Figure 2)**.

In other situations, you may need to monitor trending data without worrying about individual values. The trend chart shows overall direction without forcing you to mentally process a string of numerical outputs **(Figure 3)**.

Of course, with all these displays, if you do need precise answers at any point, individual data points and different analysis and display formats are easy to access from the front panel as well.

Simpler ways to document and distribute data

From screen captures to raw data, today's instruments make it easy to document tests and share results. For example, if you want to move the results of a data logging session to a spreadsheet, the 34461A can save the data in a .csv file that you can transfer via USB drive or over a USB or LAN connection. The LAN connection also lets you control and access the DMM—including viewing its front panel display live—from any device with a web browser.

To see how modern instruments such as the 34461A can help out on your bench, visit **www.agilent.com/find/Truevolt**
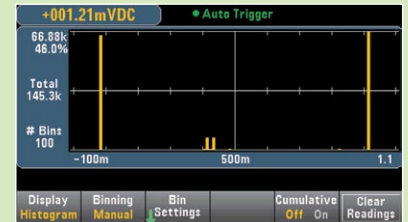
FIGURE 1.
A built-in histogram can catch anomalous events that are hard to find with other techniques.
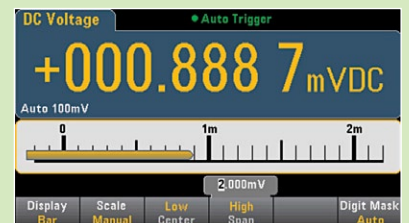
FIGURE 2.
A bar meter display offers an instant, at-a-glance qualitative view of a test or measurement.
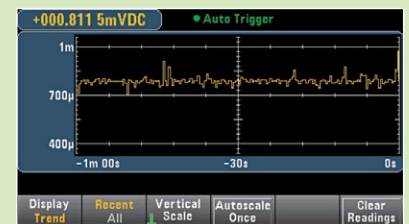
FIGURE 3.
A trend chart shows changes in measured values over time.

Agilent 34461A *- 6½ Digital Multimeter*

Benchtop DMMs

Exceptional performance and ease of use

- 4½ to 6½ digits
- Up to 50 K readings/sec
- Digital Multimeter (DMM) Connectivity Utility lets you easily control, capture and view the DMM data on your PC or mobile device

NEW **NEW** **NEW**

Model	Description	Digits of resolution	Measurement speed (rdg/sec)	Basic measurements (all AC measurements are true RMS)	Connectivity & software
U3401A U3402A	Dual display. Elegantly simple and affordable DMMs with basic capabilities	4½ (U3401A) 5½ (U3402A)	N/A	DCV, ACV, DCI, ACI, 2-wire resistance (and 4-wire resistance for U3402A), frequency, continuity, diode test	N/A
U3606A	DMM and DC power supply in one box. Halves bench/rackspace need for two instruments	5½	37	DCV, ACV, DCI, ACI, 2- and 4-wire resistance, capacitance, frequency, diode test, continuity. 30 W dual-range output 30 V/1 A and 8 V/3 A with OVP/OCP, auto scan/ramp and square wave generator	USB 2.0, GPIB
34450A	Faster measurement speed, ultra-bright OLED with dual display, and basic statistical tools	5½	190	DCV, ACV, DCI, ACI, 2- and 4-wire resistance, capacitance, frequency, continuity, diode test, temperature	USB 2.0, RS-232, optional GPIB*
34460A 34461A	Display DMM results in ways you never have before and measure with unquestioned True*volt* confidence	6½	300 *(34460A)* 1,000 *(34461A)*	DCV, ACV, DCI, ACI, 2- and 4-wire resistance, frequency & period, continuity, diode test, temperature	USB 2.0, LAN (LXI Core) (34460A optional), optional GPIB*
34401A	Industry standard for accuracy, speed, measurement ease and versatility	6½	1000	DCV, ACV, DCI, ACI, 2- and 4-wire resistance, frequency & period, continuity, diode test	GPIB, RS-232, Intuilink software support*
34410A 34411A	Dual display. Highest through-put of benchtop DMMs, best choice for system use	6½	10,000 (for 34410A) 50,000 (for 34411A)	DCV, ACV, DCI, ACI, 2- and 4-wire resistance, frequency & period, continuity, diode test, capacitance, temperature	LAN (LXI Core), USB 2.0, GPIB, Intuilink software support*

See **PROMO** Page 2 **NEW**

*New DMM Connectivity Utility Software available

Handheld DMMs

Rich features and robust design for real-world conditions

- High-contrast OLED display with 160° viewing angle (U1273AX, U1273A and U1253B)
- CAT III 1000 V and CAT IV 600 V over voltage protection (U1240, U1250, and U1270 Series)
- Large 2 inch jaw size with high measurement capability of up to 1000 A for AC, DC, or AC+DC (U1210 Series)

The U1177A
Infrared (IR)-to-*Bluetooth*® Adapter:
Enables *Bluetooth* connection to ALL Agilent U1200 Series handheld DMMs. Use with the complimentary Agilent application software, Mobile Meter and Mobile Logger, on your Android device to monitor and log data remotely and wirelessly (of up to 3 HH DMMs).

Agilent U1177A: an electronics industry multiple award winner for 2013.

	U1230 Series	U1240 Series	U1250 Series	U1270 Series	U1210 Clamp Meter Series
Counts	6,000	10,000	50,000	30,000	4,000
AC bandwidth	1 kHz	2 kHz	30 to 100 kHz	100 kHz	2 kHz
Voltage AC/DC	600 mV to 600 V	1 to 1,000 V	50 mV to 1,000 V	30 mV to 1,000 V*	4 to 1,000 V
Current AC/DC	60 µA to 10 A	1 mA to 10 A	500 µA to 10 A	300 µA to 10 A	40 to 1,000 A
Battery life	500 hours	300 hours	72 hours*	300 hours	60 hours
Additional features	Built-in flashlight, continuity alert with flashing backlight, Z_{Low} Non-contact voltage detector with V_{sense}*	Switch counter, harmonic ratio, dual and differential temperature measurements*	20 MHz frequency counter, programmable square wave generator*	Low pass filter. AC and/or DC voltage check, low impendance mode offset compensation* Operational down to -40 °C*	Large 2″ jaw size, back light with dual display, ACI, ACV/DCV, Diode, R, C, Frequency 400 Ω to 40 M Ω Resistance 400 to 4,000 µF Capacitance
Connectivity	IR-USB and *Bluetooth*	IR-USB and *Bluetooth*	IR-USB and *Bluetooth*	IR-USB and *Bluetooth*	*Bluetooth*

*Specification available on select models only.

Breakthrough scope technology lets you see more, do more and get more for your money

1000 Series oscilloscopes

1000B series now reduced in price

- 50 to 200 MHz, 2 and 4 channel DSO models with up to 20 kpts memory
- 5.7-inch color display offers powerful signal capture and display
- Up to 2 GSa/s sample rate
- 23 automatic measurements, sequential acquisition, mask testing and digital filters
- 11-language user interface, USB connectivity, and a standard educator's kit

InfiniiVision 2000 X-Series oscilloscopes

See PROMO Page 2

- 70 to 200 MHz bandwidth, up to 1 Mpts memory, DSO and MSO models
- Up to 50,000 waveform updates/second
- 8.5-inch WVGA display offers 2x the viewing area and 5x the resolution of competitive scopes
- Fully upgradable—bandwidth, MSO, memory, serial analysis, WaveGen built-in 20 MHz function generator, and integrated digital voltmeter

InfiniiVision 3000 X-Series oscilloscopes

See PROMO Page 2

- 100 MHz to 1 GHz bandwidth, up to 4 Mpts memory, DSO and MSO models
- Up to 1,000,000 waveform updates/second
- 8.5-inch WVGA display is 50% larger and 3x the resolution of competitive scopes
- Mega*Zoom* IV responsive, uncompromised smart memory with segmented memory optional
- Fully upgradable—bandwidth, MSO, memory, WaveGen built-in 20 MHz arb/function generator, integrated digital voltmeter, and serial analysis

InfiniiVision 4000 X-Series oscilloscopes

NEW

See PROMO Page 2

- 200 MHz to 1.5 GHz bandwidth, bandwidth, 4 Mpts smart memory, DSO and MSO models
- Up to 1,000,000 waveform updates/sec
- 12.1-inch capacitve touch display— 40% larger than competitive scopes
- Industry's only InfiniiScan Zone touch triggering
- Mega*Zoom* IV uncompromised smart memory with segmented memory standard
- Fully upgradable—WaveGen built-in 20 MHz arb/function generator, integrated digital voltmeter, and serial analysis including USB

Gain greater insight with powerful applications

See the complete list at www.agilent.com/find/scope-apps

Description	2000 X-Series	3000 X-Series	4000 X-Series
20 MHz WaveGen	DSOX2WAVEGEN	DSOX3WAVEGEN	DSOX4WAVEGEN2 2-ch AWG
3-digit voltmeter	DSOXDVM	DSOXDVM	DSOXDVM
DSO to MSO upgrade	DSOX2MSO	DSOX3MSO*	DSOXPERFMSO
NEW CAN/LIN trigger/decode	DSOX2AUTO	DSOX3AUTO	DSOX4AUTO
NEW I²C/SPI trigger/decode	DSOX2EMBD	DSOX3EMBD	DSOX4EMBD
NEW RS232/UART trigger/decode	DSOX2COMP	DSOX3COMP	DSOX4COMP
NEW USB full/low trigger/decode			DSOX4USBFL
NEW USB high trigger/decode			DSOX4USBH
NEW USB signal quality test			DSOX4USBSQ

1 GHz models require DSOXPERFMSO

Get a FREE 30-Day Trial License. **www.agilent.com/find/30daytrial**

Maximum versatility to troubleshoot today's challenges and anticipate tomorrow's needs

U1600 Series handheld scopes

See PROMO Page 2

- 5.7-inch VGA TFT LCD display with indoor, outdoor, and night-vision viewing modes
- 3-in-1 instrument: scope, DMM, and data logger
- Two independent, isolated channels (U1610A, U1620A)
- Up to 2 GSa/s sample rate and up to 2 Mpts deep memory to zoom in on critical details
- Benchtop-like dual window zoom for more detailed waveform analysis

Achieve deep insights quickly with histograms, trend charts and statistics

RF and universal frequency counters
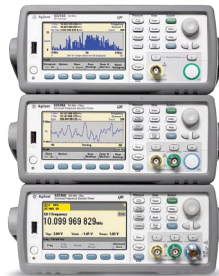
- Frequency, frequency ratio, time interval, rise/fall time, phase, and much more
- Histograms, trending, data logging, and built-in math and statistics functions give greater insights into system behavior
- 53230A offers: 20 ps single-shot, burst microwave, and continuous gap free measurements with time stamped edges.
- Optional 6 or 15 GHz RF channel
- USB, GPIB and LAN (LXI Core) connectivity

Model	Key specifications
53210A	350 MHz RF frequency counter, 10 digits/s
53220A	350 MHz universal frequency counter/timer, 12 digits/s, 100 ps
53230A	350 MHz universal frequency counter/timer, 12 digits/s, 20 ps

Easy connections

82350B PCI high-performance GPIB interface

- Easily control instruments and exchange data with maximum throughput, and comes with built-in buffering for speeds up to 900 KB/s.

82357B USB/GPIB interface

- Comes with high-speed USB 2.0 with fast, easy, plug-and-play connection and auto configuration, and offers a GPIB transfer rate of up to 1.15 MB/s

E5810B LAN/GPIB/USB Gateway

- Remote access and control GPIB, USB and RS-232 instruments over LAN
- Faster GPIB transfer rate: 1.2 MB/s
- Easy setup and use via LCD display
- 1000BASE-T/100BASE-TX/10BASE-T LAN compatibility

SIGNAL GENERATORS
SPECTRUM/SIGNAL ANALYZERS
DATA ACQUISITION/SWITCH UNITS

WAVEFORM GENERATORS
MODULAR INSTRUMENTS
LCR METER

Achieve more on a tight budget: Solid performance with robust measurement features

N9310A RF signal generator

- 9 kHz to 3 GHz CW output, 20 Hz to 80 kHz low frequency (LF) output
- -127 to +13 dBm output level range (max +20 dBm settable)
- - 95 dBc/Hz SSB phase noise
- Extensive analog modulation: AM, FM, phase, and pulse modulation
- Optional IQ modulator, 20 MHz bandwidth
- Up to +/- 0.1 ppm aging rate

N9320B RF spectrum analyzer

- PowerSuite: high-confidence answers with simple one-button measurements of channel power, occupied bandwidth and other key parameters
- AM/FM and ASK/FSK demodulation analysis
- LAN, GPIB, and USB connectivity
- Frequency range: 9 kHz to 3 GHz
- DANL: -148 dBm with pre-amp on
- RBW: 10 Hz to 1 MHz
- Free remote control PC software

N9322C RF spectrum analyzer

NEW

- Frequency range: 9 kHz to 7 GHz
- DANL: -152 dBm typical, with preamp on
- RBW: 10 Hz to 3 MHz
- Sweep time: 2 ms to 1000 s
- 7 GHz tracking generator, built-in VSWR bridge
- AM/FM, ASK/FSK demodulation
- Free remote control PC software

Modular flexibility and universal channels for a wide range of measurements with no external signal conditioning

34970A/72A data acquisition switch unit

See PROMO Page 2

- Low cost, 3-slot unit with 6½ digit DMM and built-in signal conditioning
- Choose from 8 plug-in modules, up to 120 1- wire (60 2-wire) channels or 96 cross points
- Benchlink Data Logger software included, optional 34830A Benchlink Data Logger Pro
- GPIB & RS-232 connectivity (34970A) USB & LAN (LXI Core) connectivity (34972A)—built-in web interface for easy control

34970A/72A plug-in modules

Model	Key specifications
34901A/02A/08A multiplexers	Up to 300 V, 16, 20, or 40 channels
34903A GP switch	300 V, 20 actuator channels
34904A matrix	4x8 matrix
34905A/06A RF switches	2 GHz dual, 50 and 75 Ω
34907A multi-function	DIO, DAC, totalizer

Validate your most challenging designs with realistic test signals using exclusive True*form* technology

33500B Series waveform generators

- Exclusive new Trueform waveform technology generates signals with the lowest jitter (<40 ps) and harmonic distortion (<0.04% THD) from 1 µHz up to 30 MHz
- Arbitrary waveforms: 1 M (16 M optional) points, sequencing, and embedded editor
- Function generator: sine, square, ramp, triangle, noise, DC, AM, FM, PWM, sum, PRBS, and more
- 16 bits of resolution, 1 mVpp to 10 Vpp
- USB, GPIB and LAN (LXI Core) connectivity

Model	Key specifications
33500B Series	20 & 30 MHz, 16-bit, 250 Msa/s, 1 M point arb
33509B/33511B	20 MHz, 1-Ch (optional arb) / (built-in arb), 20 MHz pulse
33510B/33512B	20 MHz, 2-Ch (optional arb) / (built-in arb), 20 MHz pulse
33519B/33521B	30 MHz, 1-Ch (optional arb) / (built-in arb), 30 MHz pulse
33520B/33522B	30 MHz, 2-Ch (optional arb) / (built-in arb), 30 MHz pulse
33210A	10 MHz, 1-Ch, 14-bit, 50 MSa/s, 8 K point (optional arb)
33220A	20 MHz, 1-Ch, 14-bit, 50 MSa/s, 64 K point, 5 MHz pulse
33250A	80 MHz, 1-Ch, 12-bit, 200 MSa/s, 64 K point, 50 MHz pulse
33502A	Isolated amplifier, dual channel, 50 V peak-to-peak
33503A	BenchLink Waveform Builder Pro Software

Anticipate every new challenge with reconfigurable portable test systems

USB modular instruments and data acquisition

- Mix and match the USB modular instruments, DAQ modules or switching I/O units to meet your measurement needs
- Instrument and DAQ modules can be used standalone or integrated together in the USB modular chassis
- Hi-speed USB 2.0 interfaces for easy setup, plug-and-play, and hot swappable connectivity
- U2781A USB modular product chassis can host up to six modules and synchronize multiple instruments
- Bundled Agilent Measurement Manager lets you configure and control a system with no programming

USB modular instruments (U2700 Series) includes 100/200 MHz oscilloscopes, 3-channel source measurement unit, 5 ½ digit DMM, switch matrix, and function generator. For more information, go to **www.agilent.com/find/usbmodular**

USB modular data acquisition (U2300 Series and U2500 Series) includes multifunction and simultaneous sampling multifunction DAQ devices. Additional I/O devices and RF switch driver are also available. For more information, go to **www.agilent.com/find/usbdaq**

The cost-effective way to accelerate production line LCR testing and improve component evaluation

4263B LCR meter

- 100 Hz to 100 kHz
- 0.1% basic accuracy
- High-speed measurement: 25 ms
- 6 test frequencies: 100 Hz, 120 Hz, 1, 10, 20, 100 kHz

High performance

Anticipate new demands with modular versatility, deep accuracy, and high speed

**N6700
low-profile
modular
power system**

- Ideal DC power supply solution for automated test systems: small, fast, and flexible
- Small 1 U high mainframe (400, 600, 1200 W) with slots for up to 4 programmable DC power modules
- Industry leading fast command processing time (<1 ms) to improve throughput
- Mix and match the performance you need with your choice of over 30 programmable DC power modules: basic, high performance, and precision (mA and µA); available in 50, 100, 300, and 500 W
- USB, GPIB and LAN (LXI Core) connectivity

**N6705B DC
power analyzer**

See PROMO Page 2

- Get deep insight into DUT power consumption—without assembling a complex test system
- Integrate up to four DC programmable power modules with DMM, scope, arb, and data logger features; up to 600 W total power
- USB, GPIB and LAN (LXI Core) connectivity

**6600 Series
high-performance
DC supplies**

- Fast, low-noise outputs improve measurement accuracy and test throughout
- 40 to 6600 W, single output, up to 120 V, and up to 875 A
- Programmability and built-in V & I measurements simplify test setups
- GPIB connectivity

**N3300 DC
electronic load
mainframe**

- Stable and accurate: these loads are easy to integrate into your test system
- Automated command list execution reduces workload on system controller
- 1800 W mainframe accepts up to six 150 to 600 W modules for simultaneous testing
- Maximum inputs up to 240 V and 120 A
- GPIB connectivity

Agilent offers more than

250 power products to meet your specific needs.

The free Agilent Power Product Selection Guide helps you choose your instrument by the number of outputs, output power characteristics, packaging, special features and application specific solutions.

www.agilent.com/find/powerbrochuredisty

Solid performance and robust features help you achieve more on lower budgets

**N5700 and
N8700 Series
system DC power**

- Basic, high-power, single output power supplies
- 45 affordable models in compact 1U (750 and 1500 W) and 2U (3.3 and 5 kW) packages
- Up to 600 V or up to 400 A
- Programmability and built-in V & I measurements simplify test set ups
- USB, GPIB and LAN (LXI Core) connectivity

**E3600 Series
DC power**

- Output noise as low as 1 mVp-p/0.2 mVrms
- Tight 0.01% load and line regulation
- Fast load transient response time (<50 µs)
- 30 to 200 W outputs

**U8000 Series
DC power supplies**

- Output sequencing (for U803x Series)
- Low output noise (as low as 1 mVrms) minimizes interference into your device-under-test (DUT)
- Fast load transient response time (< 50 µs) reduces test time and manufacturing cost
- Excellent 0.01% load and line regulation for steady output power levels
- Total power of 375 W at three outputs (for U803x Series)

**6030 Series
basic autoranging
DC supplies**

- Autoranging to do the job of multiple power supplies
- 240 or 1200 W output, up to 500 V and up to 120 A
- Programmability and built-in V & I measurements simplify test setups
- GPIB connectivity

Quickly and accurately evaluate your DUTs with precision/low-noise sourcing and easy-to-use GUI

**B2900A Series
source measure
units**

- Superior Graphical User Interface (GUI)
- High sourcing and measurement resolution
- Wide output range (210 V / 3 A DC / 10.5 A pulse)

**B2960A Series
low-noise power
sources**

See PROMO Page 2

- Ultra-low noise performance with the external low noise filter (10 µVrms)
- High sourcing resolution (6.5 digit, 100 nV/10 fA)
- Innovative sourcing capability and superior GUI

Capturing ghosts: the oscilloscope capabilities that matter the most

Flickering "waveform ghosts," those classic intermittent signals, are among the toughest troubleshooting challenges, so it's vital to understand how scope performance affects your ability to capture, identify, and fix these difficult creatures:

- **Real-time bandwidth and sample rate**
  These are the most important oscilloscope specifications to consider because they determine the level of detail in which signals can be captured.

- **Memory depth and display update rate**
  Deep memory is a powerful tool for catching ghosts because it lets you sample at higher rates over a longer period of time, and a fast display system greatly enhances a scope's ability to make those occasional waveform ghosts more visible.

- **Zone triggering**
  Using advanced parametric/violation triggering modes is sometimes easier said than done. A simpler alternative in many cases is zone triggering. Simply draw a box around the area of the ghost, and the scope will display only the anomalous waveforms that intersect that zone.

To learn more about capturing elusive signals with today's advanced scopes, **visit www.agilent.com/find/4000X-Series**
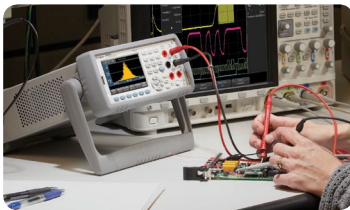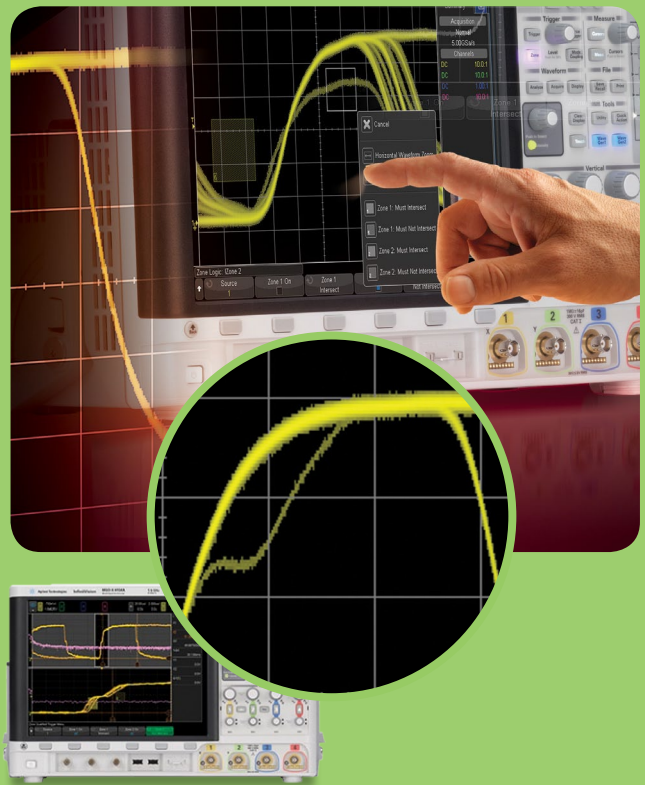
See how DMMs that do more and display more can change the way you work.

SEE PAGE 3

Anticipate ___Accelerate ___Achieve

Agilent Technologies

BY DAVID GILBERT, LINEAR TECHNOLOGY

MINIMISE STANDBY CURRENT IN AUTOMOTIVE DDR SUPPLIES

When you turn on a laptop or a smart phone, you expect to wait for it to boot up, but you are less patient when you turn on your car. With a car, consumers expect immediate access to computer electronics, including navigation and infotainment systems, and automobile manufacturers strive to meet this desire with design strategies that shorten start-up time.

One such strategy is to keep dynamic memory (RAM) active at all times, even during the ignition-off state. The DDR3 memory used in automobiles operates on a 1.5V rail with peak load currents over 2A—preferably produced by a high efficiency DC/DC converter to minimise heat dissipation. In these applications, light load efficiency is just as important to preserve battery life when the car is not running. DDR memory can consume 1 mA–10 mA from the 1.5V rail in standby, but drawing 10 mA from the battery is unacceptable when the car is parked for long periods.

This constraint rules out the use of a linear regulator, where input and output current are equal. On the other hand, a switching step-down (buck) regulator draws less input current than load current in proportion to the step-down ratio:

$$I_{IN} = \frac{1}{\eta} \bullet \frac{V_{OUT} \bullet I_{OUT}}{V_{IN}}$$

where η is the efficiency factor (0 to 1).

$V_{IN} = 12V$
$V_{OUT} = 1.5V$
$R_T = 93.1k$ (475kHz)
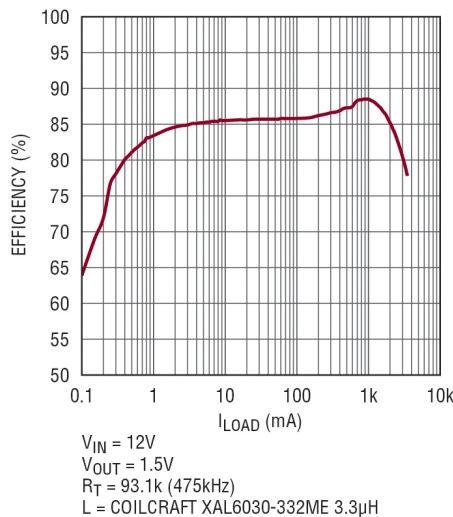L = COILCRAFT XAL6030-332ME 3.3µH

Figure 1. *LT8610AB efficiency versus load*

Figure 1 shows that the LT8610AB synchronous step-down regulator achieves around 83% efficiency at a 1 mA load. For a battery voltage of 12V and load current of 1 mA at 1.5V, calculated input current is only 151 µA.

12V CAR SUPPLY TO 1.5V DDR

When the task is to carry out direct DC/DC conversion from a car battery to 1.5V DDR memory, a solution lies with LT8610A and LT8610AB which are monolithic, synchronous step-down regulators designed specifically for automotive systems. They deliver 3.5A while consuming only 2.5 µA quiescent current. Building a circuit around them is straightforward as no addi-
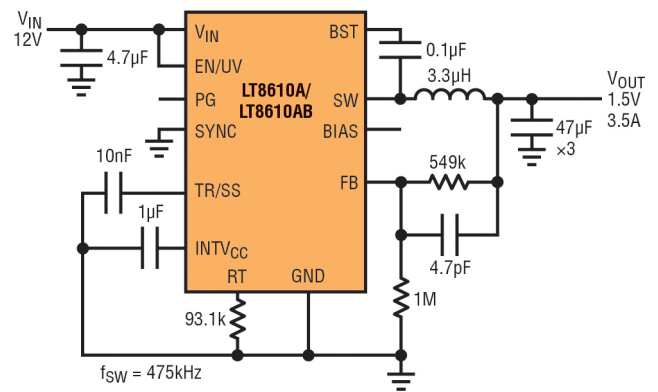

Figure 2. *This step-down converter circuit accepts automotive battery and generates 1.5V at 3.5A. Low quiescent current and synchronous rectification result in high efficiency across the entire load range.*

tional semiconductors are required, they work with inexpensive ceramic capacitors, and the MSOP package has leads that are easy to solder and inspect. With a typical minimum on-time of 30 nsec (45 nsec guaranteed maximum), you can design compact, high switching-frequency buck regulators with large step-down ratios. Figure 2 shows an application that delivers 3.5A at 1.5V. The operating frequency is 475 kHz to optimise efficiency and remain below the AM radio band.
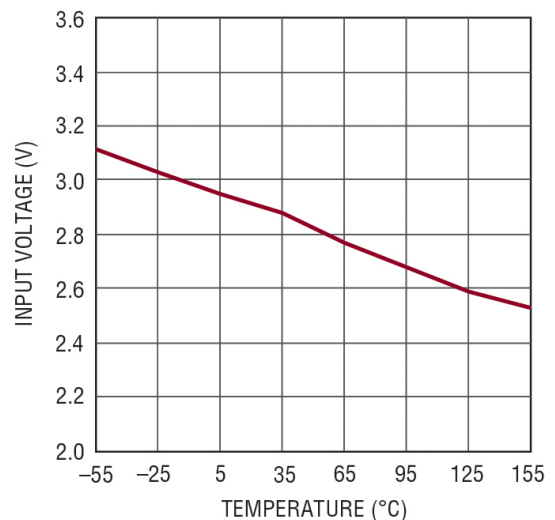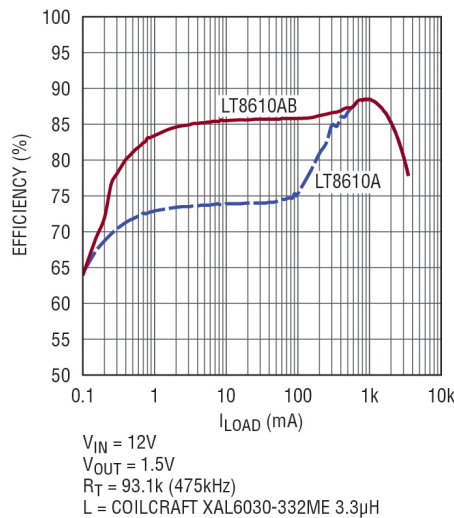

Figure 3. *Keeping the memory alive in cold-crank or start-stop events, operation is down to a typical minimum input voltage of 2.9V at 25°C, with 3.4V maximum guaranteed over temperature.*
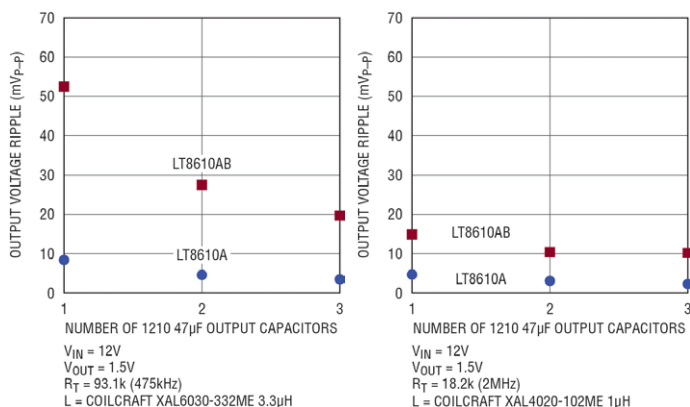
V_{IN} = 12V
V_{OUT} = 1.5V
R_T = 93.1k (475kHz)
L = COILCRAFT XAL6030-332ME 3.3µH

Figure 4. *An increased Burst Mode current limit on the LT-8610AB results in substantial efficiency gains at light load compared to the LT8610A.*

Both parts feature excellent fault tolerance to automotive environments. A maximum input of 42V handles load dumps. A robust switch design and high speed current comparator protect the device during output shorts. The minimum input is worst-case 3.4V, the maximum duty cycle is above 99% and the dropout voltage is typically 200 mV at 1A, all of which keep the output in regulation through cold-crank. The typical minimum input voltage is plotted in Figure 3.

CONSERVING BATTERY CHARGE

A major part of the designer's task is to avoid discharging the battery, to which low ripple burst mode operation and minimal quiescent current both contribute. The LT8610A and LT8610AB are designed to minimise output voltage ripple over the entire load range. At light loads, they maintain efficiency by reducing their operating frequency and entering Burst Mode operation. Fast transient response is maintained even at very low loads. This feature combined with the very low quiescent current of 2.5 µA means that, even at a few µA of load, the converters are more efficient than a linear regulator with zero quiescent current. For systems where low frequency operation must be avoided, Burst Mode operation can be turned off by applying either a logic high signal or clock signal to the SYNC pin.

(a)
V_{IN} = 12V
V_{OUT} = 1.5V
R_T = 93.1k (475kHz)
L = COILCRAFT XAL6030-332ME 3.3µH

(b)
V_{IN} = 12V
V_{OUT} = 1.5V
R_T = 18.2k (2MHz)
L = COILCRAFT XAL4020-102ME 1µH

Figure 5. *Output voltage ripple versus number of 1210 size 47 µF output capacitors for two inductor values, at 10 mA load. (a) Ripple for the 475 kHz application in Figure 2. (b) Ripple for the 2 MHz application in Figure 6.*

f_{SW} = 2MHz
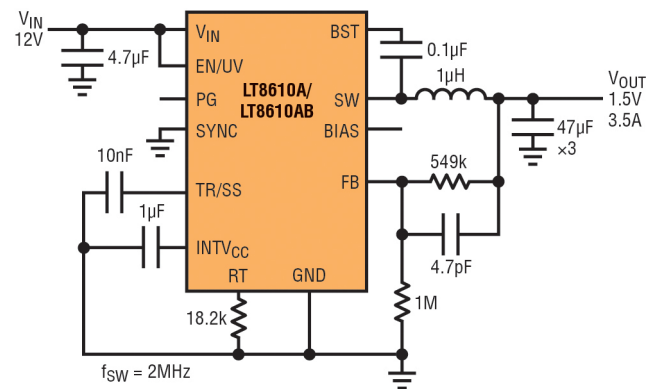
Figure 6. *Similar 12V to 1.5V application as in Figure 2, but the operating frequency is increased to 2 MHz for reduced inductor value and size.*

The difference between the two parts is that the LT8610AB features higher efficiency at light loads. This is achieved by using an increased Burst Mode current limit, allowing more energy to be delivered during each switch cycle and lowering the switching frequency for a given load. Because a fixed amount of energy is required to switch the MOSFET on and off, a lower switching frequency reduces gate-charge losses and increases efficiency.

Figure 4 shows the efficiency difference between the two parts. For loads between 1 mA and 100 mA, the LT8610AB improves efficiency by more than 10% compared to the LT8610A. The trade-off to the increased Burst Mode current limit is that more energy is delivered in each switch cycle, so more output capacitance is required to keep output voltage ripple low. Figure 5 compares the output ripple for the LT8610A and LT8610AB as a function of the output capacitance for two inductor values, at 10mA load.

In addition to the current limit, the inductor choice affects the efficiency and switching frequency in Burst Mode operation. This is because for a fixed current limit, a larger inductor value can store more energy than a smaller one. If high efficiency at light loads is paramount, then the inductor value can be increased beyond the starting value recommended in the data sheet.

FASTER, SMALLER SOLUTIONS

For most automotive systems, 9V to 16V is the typical input

LT8610AB
V_{IN} = 12V
V_{OUT} = 1.5V
R_T = 18.2k (2MHz)

LT8610A
V_{IN} = 12V
V_{OUT} = 1.5V
R_T = 18.2k (2MHz)
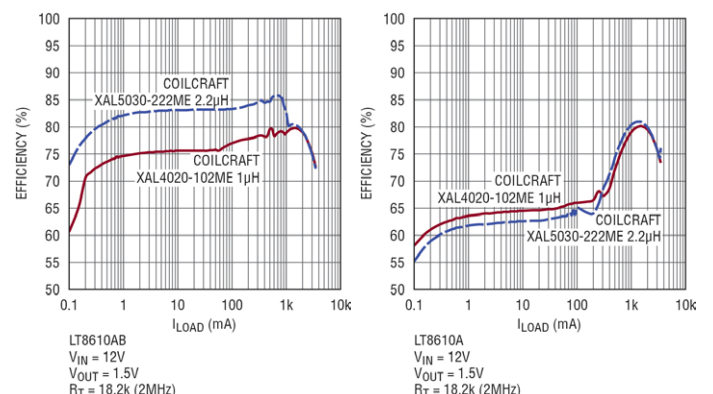
Figure 7. *Efficiency versus load at 2 MHz with two inductor values.*
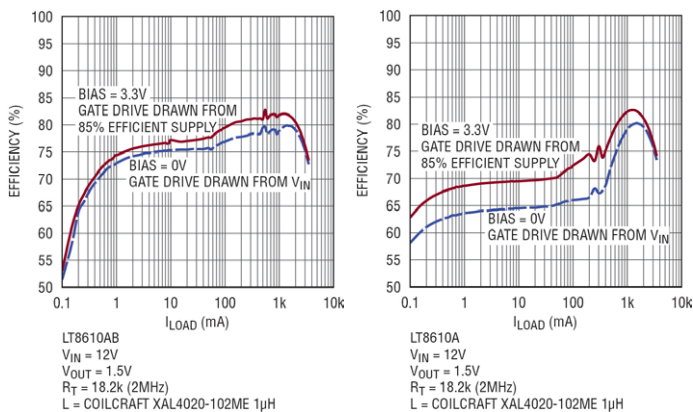
Figure 8. *Efficiency can be increased if the Bias pin is tied to an external 3.3V supply. (External supply efficiency of 85% is assumed and factored into overall efficiency shown here.)*

voltage, so application circuits are usually optimised for this range. The 475 kHz application in Figure 2 operates at the designed frequency over the entire input range of 3.5V to 42V. However, if we restrict the normal operating voltage to 16V (42V transient), the operating frequency can be increased and the value and size of the inductor reduced. With a worst-case minimum on-time of 45 nsec, the LT8610A and LT8610AB can be programmed to 2 MHz as shown in Figure 6.

Note that when the input voltage goes above 16V, the output remains in regulation although the switching frequency decreases to maintain safe operation. The 2 MHz solution is identical to the circuit in Figure 2, except for the RT resistor changed to 18.2 kΩ and the inductor value and size reduced in order to save space. Figure 7 shows efficiency versus load for two inductor choices.

BIAS PIN OPTIMISES EFFICIENCY

The LT8610A and LT8610AB use two internal nMOSFETs specifically optimised for automotive applications. In particular, the gate drive circuitry requires less than 3V to fully enhance the FETs. To generate the gate drive supply, the LT8610A/AB
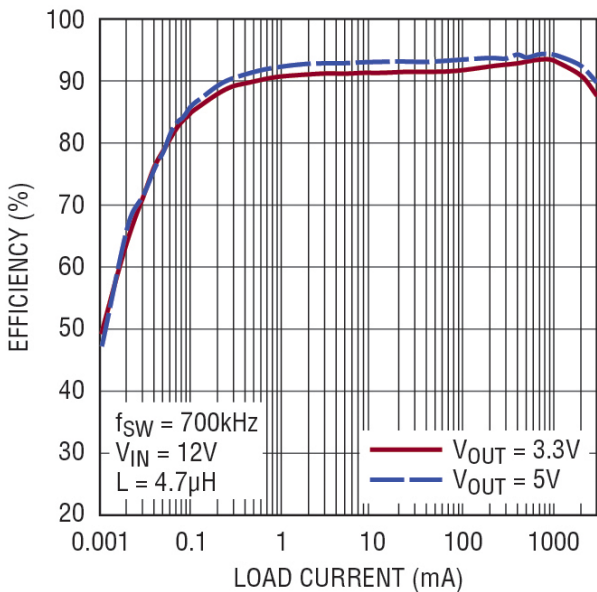
Figure 9. *Efficiency for 3.3V and 5V outputs is above 90%, reducing total power dissipation and keeping temperature under control.*
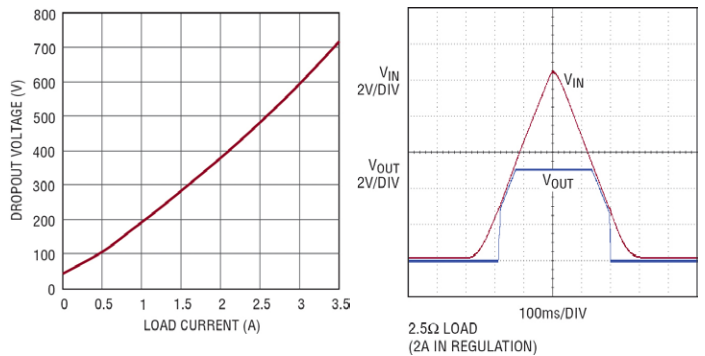
Figure 10. *The LT8610AB operates to 99% duty cycle, providing smooth start-up and low dropout voltage.*

includes an internal linear voltage regulator, the output of which is the INTVCC pin (do not load INTVCC with external circuitry).

An important feature is that this internal regulator can draw current from either the VIN pin or the BIAS pin. If the BIAS pin is left open, then gate drive current is drawn from VIN. However, if a voltage of 3.1V or higher is tied to the BIAS pin, gate drive current is drawn from BIAS. If the BIAS voltage is lower than VIN, the internal linear regulator will run more efficiently using the lower voltage supply, thus increasing overall efficiency.

The efficiency data in Figures 1, 4 and 7 was recorded with the BIAS pin open. After all, if the 1.5V output is the only rail alive, then there is likely no good place to tie the BIAS pin. However, if there is a 3.3V or 5V supply, tie it to the BIAS pin, even if the supply is not available in standby or ignition-off conditions. Figure 8 shows the efficiency with and without a 3.3V supply connected to BIAS. In calculating the total efficiency, we have included the power drawn from the 3.3V rail and assumed that it was generated with 85% efficiency.

Note that the benefit to externally powering BIAS is greater at higher operating frequencies because the gate drive current is higher. The LT8610A also benefits more from external bias compared to the LT8610AB—the AB's increased Burst Mode current limit results in a lower operating frequency for a given load.

NOT JUST FOR MEMORY

This configuration is an excellent regulator for other automotive supplies, including 3.3V and 5V supplies, with efficiency above 90%, as shown in Figure 9.

An important consideration for automotive applications is the behaviour of the power supply during cold crank and idle-stop transients, when the voltage from the 12V battery may drop below 4V. The LT8610AB operates up to 99% duty cycle, providing output regulation at the lowest possible input voltage. Figure 10(a) shows the dropout voltage. This is the difference between VIN and VOUT as the input voltage decreases towards the intended output regulation voltage. The LT8610AB also has excellent start-up and dropout behaviour, resulting in predictable and reliable output voltage as a function of input voltage. Figure 10(b) shows the output voltage as the input supply is ramped from zero to 10V and back to zero.

These devices, defined with the automotive environment in mind, have a low component count, low minimum input voltage, low quiescent current and high efficiency across a wide load range. These features suit them as solutions for providing standby power to DDR memory in automotive applications.

David Gilbert is Associate Design Engineer, Power Products, at Linear Technology Corp.

BY MARK SCHOLTEN, ON SEMICONDUCTOR

POWER SUPPLIES FOR AUTOMOTIVE START/STOP SYSTEMS

In order to curb fuel consumption, many automobile makers are implementing the "Start/Stop" function into their next generation of vehicles and significant numbers of such vehicles are already on the road. These systems turn off the engine when the vehicle comes to a stop and then automatically turn it back on when the foot is moved from the brake pedal to the accelerator pedal – or, in the case of a manual transmission, when the clutch pedal is depressed to re-engage gear. This helps reduce fuel consumption in city driving and stop-and-go rush hour traffic.

Such systems introduce some unique engineering challenges to the vehicle's electronics however, since the battery voltage can drop to 6.0 V or lower when the engine re-starts. In addition, typical electronic modules have a reverse polarity diode included to protect the electronics in the event the car is jump-started (bopsted) with the jumper cables accidentally reversed. This diode causes another 0.7 V drop in the battery voltage, leaving 5.3 V or less for down-stream circuitry. With many modules still requiring a 5 V supply, power sources are simple running out of headroom to operate properly.

BOOST SUPPLY

One approach is a boost supply. This takes a lower input voltage and creates a higher voltage on the output. Many suppliers are currently employing some type of boost supply at the front end of electronic modules in order for them to operate properly through dropout conditions caused by the Start/Stop system. The following article looks at various solutions available to the designer, including low dropout linear regulators, reverse battery protection schemes, and different boost options for these Start/Stop systems.

As with most engineering problems, there are a number of ways to solve an issue. If the battery voltage only drops down to 6V at the input, then the first and simplest solution is to find an extremely low drop-out linear regulator that requires less than 0.3V of headroom. This can work for modules with lower current requirements, but one soon runs out of options for modules with higher current needs.
An alternative approach is to replace the standard P-N junction diode used for reverse battery protection on the front end with either a Schottky diode or a P-channel MOSFET. A Schottky diode has about half of the forward voltage drop of a standard

Figure 1: *Reverse battery with P-FET*

rectifier, so it adds a few more tenths of a volt to the headroom. Changing to a Schottky diode is straight-forward enough, since it typically fits right onto the same PCB pads as the standard diode, eliminating the need for layout changes.
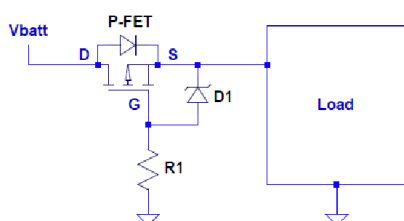
The P-channel MOSFET however requires a PCB change, along with some extra circuitry.

Figure 1 illustrates the three components that are required; a P-FET, a Zener diode, and a resistor. The P-FET needs to be sized so that it can handle the voltages applied to the input of the module, along with the load currents required. In addition, it is important to consider the thermal requirements of the system, since the power dissipation in the FET is the current squared times the on-resistance of the FET. The Zener diode protects the MOSFET's gate oxide from damage due to over-voltage conditions. Most P-FETs can handle between 15-20V from their gate to source connections, so the Zener has to be chosen to clamp before this point. The resistor pulls the gate down to ground to turn on the P-FET, but it also must be sized appropriately. It cannot have too little resistance, because then too much current will be allowed to flow through the Zener – thereby creating power dissipation issues for it. However, if it gets too large, then the P-FET may not turn on as hard as preferred, and the whole idea for this scheme is to reduce the voltage drop across the drain to source connection.

VOLTAGE DIPS TO UNDER 5V

It is likely that one, or a combination, of the above schemes, will work for a given application. But what happens if the input voltage actually drops below 5V? Some manufacturers are looking at 4.5V during "cold cranking" conditions. If this is the case, then a switching power supply needs to be used in order to boost the input voltage. The three most common switchers are the boost supply, the buck/boost supply, and the SEPIC power supply.

The boost supply uses one inductor, one N-FET, one diode, and one capacitor. It is the simplest design, but it also has some drawbacks. If the output should be shorted, there is no way to protect it because there is a direct path from the input to the output. Also, when the input voltage rises above the output voltage set point, there is nothing to keep the output from also rising, since the input voltage can go right through the inductor and diode to the output.

For example, most modules on a vehicle must pass the load dump test. In this test, a voltage spike is generated and applied to Vin. In a boost supply, this voltage spike would propagate right to the output. Thus, if a 40-V spike comes down the line, everything connected to Vout has to be able to handle this voltage.
The next possibility is the non-inverting buck/boost design. This uses only one inductor and capacitor, but it requires two switches and two diodes. The scheme however does allow a designer to keep the output voltage from rising when the input goes higher than the output. It also enables protection from output short circuits by opening up the first switch (FET1). The downside to this design is its efficiency, as now there are losses in two diodes and two switches to take into account.

The Single-Ended Primary-Inductor Converter (SEPIC) design is very similar in layout to the straight boost converter except that it adds an inductor to ground and a DC blocking capacitor. The negative side here is the addition of another inductor and capacitor, but on the positive side there are no more issues with the output being short circuited as the DC blocking capacitor is now in series with the output. The output now is not affected by the input voltage, so it can be lower or higher than the input. One thing to note is that with all of the switching topologies shown, a reverse battery protection scheme is still needed, since reverse current can still flow from ground through the body diode of the FET back to input voltage.

In summary, there are many issues to consider when going to a Start/Stop alternator system. This article has touched just on the power supplies for electronic modules, but there are also other concerns that need to be addressed. For example, both interior and exterior lighting will dim during these voltage dips. Interior lights blinking can be annoying though not critical, but brake lights and headlights directly affect safety, so these will also need power supply solutions to keep them up and running. Fortunately, there are now solutions in existence for these problems.

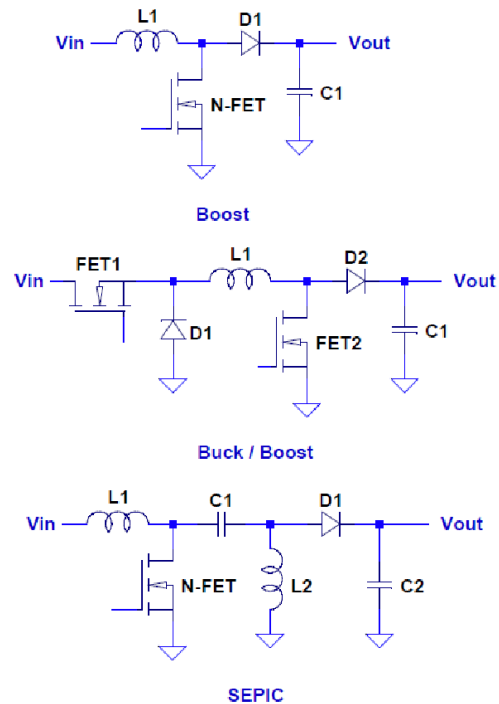**Mark Scholten is a Senior FAE with ON Semiconductor; www.onsemi.com**

Figure 2: *Various Boost Supplies*

BY JOHN CALDWELL, TEXAS INSTRUMENTS

SIGNAL DISTORTION FROM HIGH-K CERAMIC CAPACITORS

Multilayer ceramic capacitors (MLCCs) are used extensively in modern electronics because they offer high volumetric efficiencies and low equivalent series resistances at attractive prices. These advantages make MLCCs nearly ideal for a wide range of applications, including output capacitors for power supplies and local decoupling capacitors for integrated circuits. The various types of MLCCs are delineated primarily by their temperature coefficient, which is the amount of variation in their capacitance over a specified temperature range. Class I types, given a designation of NP0 or C0G, must vary less than ±30 ppm over their operating temperature range, while Class II types can change anywhere from ±15 percent (X7R) to +22 percent /–82 percent (Z5V).

C VARIES WITH T – AND WITH V

The temperature coefficient of an MLCC is a direct effect of the materials used in the ceramic that forms the capacitor dielectric. Furthermore, the dielectric material also determines the electrical characteristics of the capacitor. Class II dielectric types (X7R, Z5U, Z5V), often are referred to as "high-k" ceramics because their dielectric materials, have relative permittivities that range from 3000 (X7R) up to 18000 (Z5U). Class I C0G capacitors tend to have relative permittivities in the range of six to 200 [1]. The benefit of increased relative permittivity of the

dielectric material is that high-k MLCCs are available in much larger capacitance values and smaller packages than C0G types.

Unfortunately, these advantages come with a downside: high-K MLCCs exhibit a substantial voltage coefficient, meaning their capacitance varies depending on the applied voltage. In AC applications this phenomenon manifests itself as waveform distortion and can compromise the overall system performance. When printed circuit board (PCB) area and cost are major design constraints, board and system level designers may be tempted to use high-K MLCCs in circuits where they can introduce significant distortion into the signal path.

In the balance of this article, the author considers the origins and magnitude of unexpected distortion that may arise in this way, and presents a measurement approach to quantify it. He concludes;

Although there are many applications where high-k MLCCs are useful for engineers, it is not advisable to use them in areas of a system's signal path where significant voltage drop across the capacitor allows it to contribute distortion.

The complete article is available as a White Paper from EDN Europe's website.

BY BONNIE BAKER

Closer to real-world analogue filters

There are two basic filter topologies that everyone recommends when they start to design their signal chain: multiple-feedback (MFB) or Sallen-Key topologies. But what are the differences and why would you choose one over the other?

MFB FILTERING

The MFB topology (sometimes called infinite gain or Rauch) is often preferred because it has low sensitivity to amplifier variations, such as the open-loop gain or input range (Figure 1). The MFB topology creates a second-order filter. A MFB single-stage (second-order filter) provides two poles while inverting the signal. In designs where an even number of stages is required, such as a fourth- or eighth-order filter, the output polarity is the same as the input signal. A sixth-order filter consisting of three MFB stages inverts the signal three times, resulting in an inverted output after the third stage. This inversion may, or may not, be a concern in the application circuit, particularly if you have differential input/output stages.

In Figure 1, the gain circuit is negative and equal to the resistor ratio of R2 and R1. This arrangement allows a variety of negative gains. Generally, the MFB topology allows low sensitivity to component tolerances. The value required for C1 in an MFB design can be quite low while the designer is trying to use reasonable resistor values. The caveat is that low capacitor values can result in significant errors due to parasitic capacitance and the input capacitance of the amplifier.
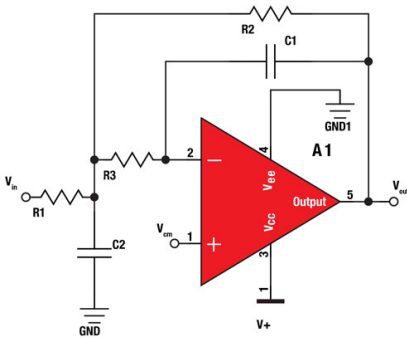
SALLEN-KEY FILTERS

There are instances where the Sallen-Key topology is a better choice. A single, second-order Sallen-Key stage also provides two poles but is a non-inverting circuit. This may be preferable over a MFB single stage, but this is not the only potential advantage. As a rule of thumb, the Sallen-Key topology is better if:

1. gain accuracy is important, and
2. a unity-gain filter is needed, and
3. a low Q is required
   (for example, Q < 3)

At unity-gain, the Sallen-Key topology has excellent gain accuracy. This is because the op amp is in a unity-gain buffer configuration with a high open-loop gain. Consequently, the gain is independent of the resistors in the circuit. With the MFB topology, the R2/R1 resistor ratio and the resistor errors determine the gain. The unity-gain Sallen-Key topology also requires fewer components—two resistors versus three for the MFB (Figure 2).

Your circuit also may require a low Q, the quality factor. The relationship between Q and the damping factor is Q = 1/2 ζ, where ζ is the damping factor. The higher the Q, the more easily the circuit oscillates, particularly at the 3-dB corner frequency.
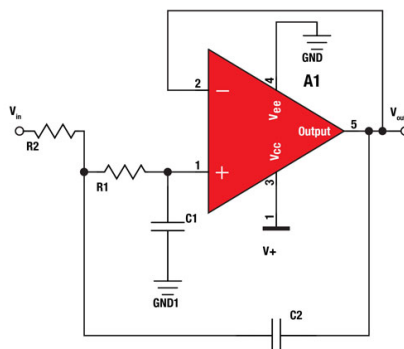
The Sallen-Key topology may be preferable for low-Q, high-frequency filter sections.

Selecting the correct amplifier, for these circuits, presents an interesting challenge. It is not simply a matter of picking an amplifier with a gain-bandwidth-product that is 100 times higher than the filter's corner frequency. The amplifier bandwidth calculation involves variations of the amplifier's bandwidth and variations of the passive components over time, to mention a few. Sometimes amplifier manufacturers, such as Texas Instruments with the WEBENCH Filter Designer Web software, provide a list of the appropriate amplifiers for the related filter. This program provides the actual amplifier suggestion, along with alternatives if you would rather use an amplifier other than the suggested device. Filter Designer also provides SPICE simulations of the chosen filter's sine wave response, step response, and closed-loop ac response.

The WEBENCH Filter Designer program seems to have broken through some filter design barriers. All I can say is filter design has come a long way, baby.

REFERENCE

1. WEBENCH Filter Designer program, Texas Instruments; http://www.ti.com/lsds/ti/analog/webench/webench-filters.page?DCMP=hpa_contributed_article&HQS=webenchfilter-cahttp://

Bonnie Baker is a senior applications engineer at Texas Instruments and author of A Baker's Dozen: Real Analog Solutions for Digital Designers.
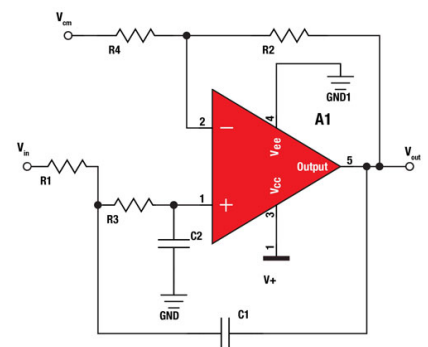

Figure 1. *MFB second-order single-supply low-pass filter. The gain of this circuit is equal to −R2/R1, where VCM=V+/2.*

Figure 2 *A Sallen-Key second-order, dual-supply, low-pass unity gain filter. The gain of this circuit is equal to 1V/V.*

Figure 3 *Sallen-Key second-order, single-supply filter. The gain of this circuit is 1+R2/R1. VCM=V+/2.*

VICOR

Solutions from **AC to Point of Load**

Our Latest Products

Picor Cool-Power Isolated ZVS DC-DC Converters

Simple to Use

- Complete Isolated DC-DC converter with zero-voltage switching module
- Three input voltage ranges for communication, industrial, rugged/M-Grade applications
- Communication converters have max peak input voltage of 100 V / 100 ms (non-operating)
- 2,250 V input to output isolation

High Density

- 50 W / 60 w output power (dependent upon converter model)
- Surface mount 22mm x 16.5mm x 6.7mm high-density package
- 900 kHz switching frequency, miminizes input filtering and reduces output capacitance

Rich Feature Set

- On/Off Control, positive logic ENABLE
- Wide trim range +10/-20% Trim
- Temperature monitor™ & Over-temperature Protection (OTP)
- Input UVLO & OVLO and output OVP
- Over current protection with auto restart
- Adjustable soft-start
- Output voltage sensing without opto coupler use for higher reliability

Resources

Blog Post: The technology behind the Cool-Power ZVS DC-DC Converters

Video: An Introduction to Vicor's Cool-Power ZVS DC-DC Converters

Cool-Power	Input	Output Set	Output Range	I_{OUT}Max
Communications (-40ºC to 125ºC)				
PI3101-00-HVIZ	36 – 75 Vin	3.3 V	3.0 to 3.6 V	18 A
PI3105-00-HVIZ		12 V	9.6 to 13.2 V	5 A
PI3110-01-HVIZ	41 – 57 Vin	18 V	16.2 to 19.8 V	3.3 A
Industrial (-40ºC to 125ºC)				
PI3109-01-HVIZ	18 – 36 Vin	5 V	4.0 to 5.5 V	10 A
PI3106-01-HVIZ		12 V	9.6 to 13.2 V	4.2 A
M-Grade (-55ºC to 125ºC)				
PI3109-00-HVMZ	16 – 50 Vin	5 V	4.0 to 5.5 V	10 A
PI3106-00-HVMZ		12 V	9.6 to 13.2 V	4.2 A
PI3111-00-HVMZ		15 V	12 to 16.5 V	3.3 A

Two-Part Web Seminar Series About EMI

Watch Part 1
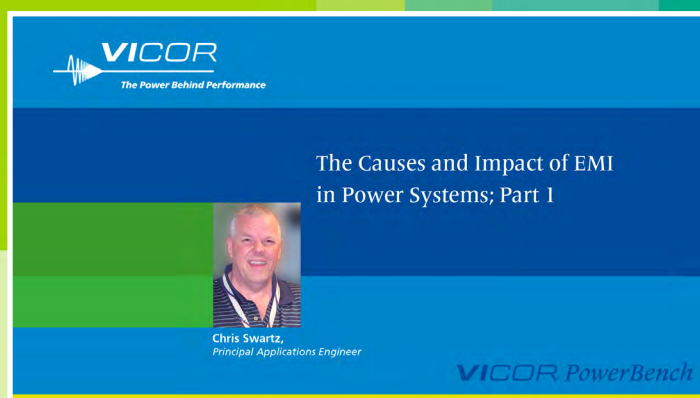
Register Now for Part 2
- to be broadcast on 18 September

The Causes and Impact of EMI in Power Systems; Part 1

Chris Swartz,
Principal Applications Engineer

VICOR PowerBench

Practical Design Con... and Solutions for the Reduc... Conducted EMI and Filter ... Power Systems; Part 2

Chris Swartz,
Principal Applications Engineer

VICOR PowerBench

Coming Soon

The Causes and Impact of EMI in Power Systems

Practical Design Considerations and Solutions for the Reduction of Conducted EMI and Filter Size in Power Systems

# VI Brick AC Front End

Overview

- Universal Input: 85 – 264 Vac
- Output: 48 Vdc - isolated, regulated (SELV)
- Power: 330 W - over entire input voltage range
- Isolated AC-DC converter with active Power Factor Correction (PFC)
- Integrated rectification, filtering and transient protection
- Peak efficiency: >92%
- EN55022, Class B EMI conducted emissions with a few components
- EN61000-3-2 harmonic limits
- -55 to 100°C baseplate operation

Features

- Low profile, 9.55 mm height above board
- Small footprint, size of a business card
- Flanged aluminum package for secure mounting and thermal management
- Consistent high efficiency across the worldwide mains (flat efficiency curve)
- Reduced power loss and cooling requirements
- Module includes PFC, regulation, isolated 48 V output (SELV), filtering, rectification, transient protection, agency approvals, simplified thermal management
- Simple design, requires few external components
- Module power density, 121 W/in³
- Complete solution including hold-up capacitors, 54 W/in³

Basic Application

9.55 mm
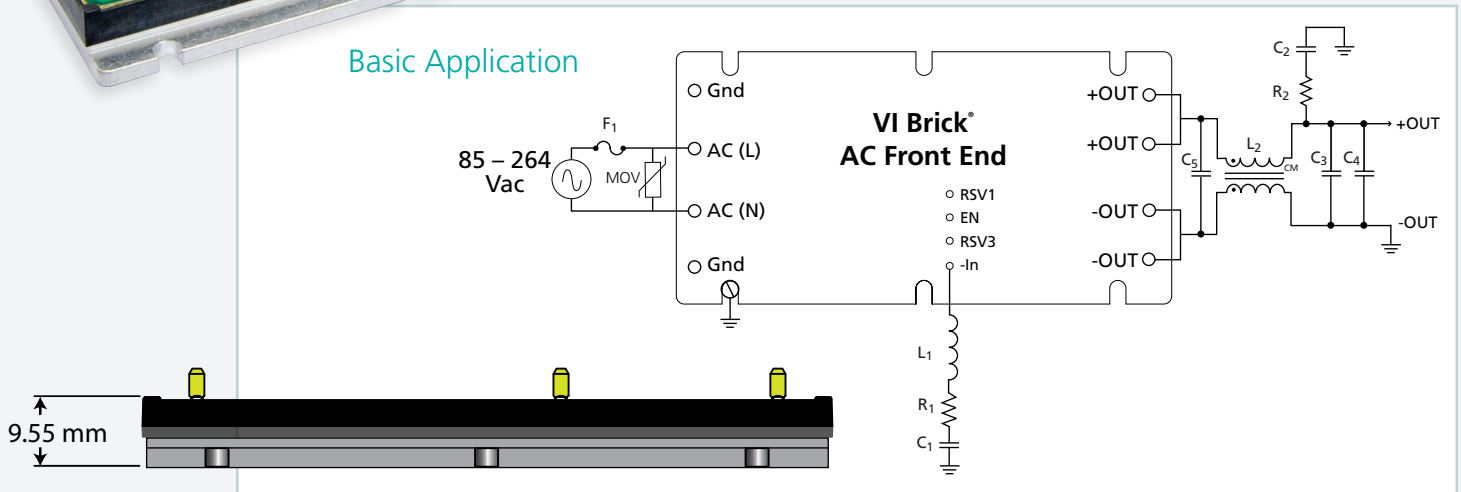
Resources

▶ An Introduction to the Vicor AC Front End Module

▶ Webinar: Designing High Performance AC-DC Power Systems Using a Power Component Approach

▤ AC Front End Product Information

Consistent High Efficiency
Over Line, Load, Temperature

Part Number	Input Voltage	Output Voltage	Output Power	Operating Temperature
FE175D480C033FP-00	85 – 264 Vac	48 Vdc	330 W	-20 to 100°C
FE175D480T033FP-00	85 – 264 Vac	48 Vdc	330 W	-40 to 100°C
FE175D480M033FP-00	85 – 264 Vac	48 Vdc	330 W	-55 to 100°C

Replace the "–00" suffix in the part number with "–CB" to order an evaluation board.
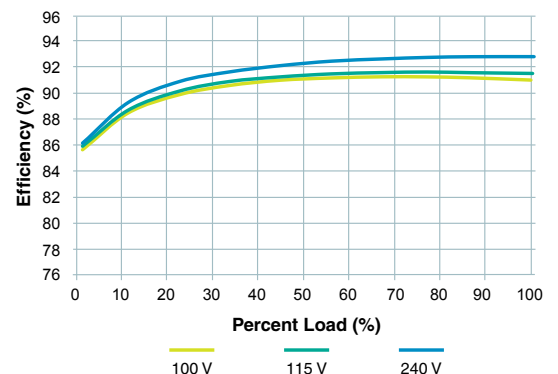
Picor Cool-Power ZVS Buck Regulators

Wide Operating Range

- Wide V_{IN} (8 – 36 V) and wide V_{OUT} (1 – 16 V)
- 12 V-optimized performance with PI34xx Series
- -40°C to 125°C operating range

## Simple to Use; Fast Development Time

- Internal compensation - few external components
- No additional design or additional settings required

High Efficiency

- Up to 98% peak efficiency (19 V_{IN} to 15 V_{OUT})
- PI34xx Series optimized for 12 V_{IN} with even higher efficiency
- Light and full load high-efficiency performance

Flexible and Rich Feature Set

- Paralleling and single wire current sharing
- Frequency synchronization
- User adjustable soft-start & tracking
- Power-up into pre-biased load
- Optional I²C functionality & programmability
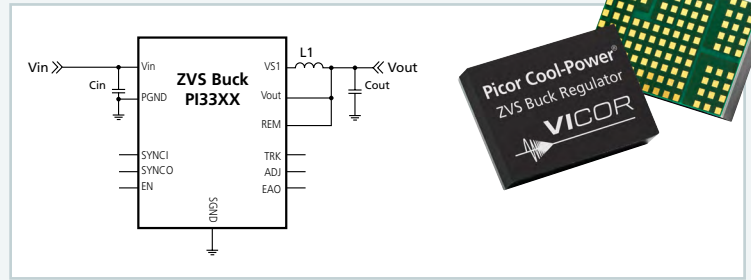
Cool-Power	Output Range		I_{OUT}
Model Number	Set	Trim Range	Max
PI3311-00-LGIZ	1.0 V	1.0 V to 1.4 V	10 A
PI3318-00-LGIZ	1.8 V	1.4 V to 2.0 V	10 A
PI3312-00-LGIZ	2.5 V	2.0 V to 3.1 V	10 A
PI3301-00-LGIZ	3.3 V	2.3 V to 4.1 V	10 A
PI3302-00-LGIZ	5.0 V	3.3 V to 6.5 V	10 A
PI3303-00-LGIZ	12 V	6.5 V to 13.0 V	8 A
PI3305-00-LGIZ	15 V	10.0 V to 16.0 V	8 A
Higher Current Versions			
PI3311-01-LGIZ	1.0 V	1.0 V to 1.4 V	15 A
PI3318-01-LGIZ	1.8 V	1.4 V to 2.0 V	15 A
PI3312-01-LGIZ	2.5 V	2.0 V to 3.1 V	15 A
PI3301-01-LGIZ	3.3 V	2.3 V to 4.1 V	15 A
I²C Functionality and Programmability			
PI3311-20-LGIZ	1.0 V	1.0 V to 1.4 V	10 A
PI3318-20-LGIZ	1.8 V	1.4 V to 2.0 V	10 A
PI3312-20-LGIZ	2.5 V	2.0 V to 3.1 V	10 A
PI3301-20-LGIZ	3.3 V	2.3 V to 4.1 V	10 A
PI3302-20-LGIZ	5.0 V	3.3 V to 6.5 V	10 A
PI3303-20-LGIZ	12 V	6.5 V to 13.0 V	8 A
PI3305-20-LGIZ	15 V	10.0 V to 16.0 V	8 A
PI3311-21-LGIZ	1.0 V	1.0 V to 1.4 V	15 A
PI3318-21-LGIZ	1.8 V	1.4 V to 2.0 V	15 A
PI3312-21-LGIZ	2.5 V	2.0 V to 3.1 V	15 A
PI3301-21-LGIZ	3.3 V	2.3 V to 4.1 V	15 A
12 V Optimized Option			
PI3420-00-LGIZ	1.0 V	1.0 V to 1.4 V	15 A
PI3421-00-LGIZ	1.8 V	1.4 V to 2.0 V	15 A
PI3422-00-LGIZ	2.5 V	2.0 V to 3.1 V	15 A
PI3423-00-LGIZ	3.3 V	2.3 V to 4.1 V	15 A
PI3424-00-LGIZ	5.0 V	3.3 V to 6.5 V	15 A

(Left bracket labels: 8 – 36 Vin for the upper groups; 8 – 18 Vin for the 12 V Optimized Option)

I²C is a trademark of NXP Semiconductors

Resources

▶ Video: Interview with ECE Europe about ZVS Regulators

▶ Webinar: ZVS Point-of-Load Regulation – Enabling High Performance On-Board Power Solutions

▶ Webinar: Design Considerations For High Performance On-Board Power Design

▤ Cool-Power ZVS Buck Regulators Product Information
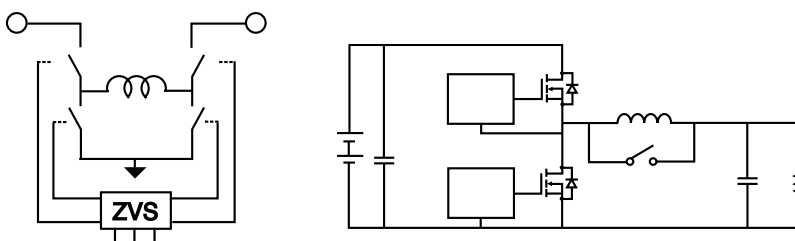
- Reduces Q1 turn-on losses
- Reduces gate drive losses
- Reduces body diode conduction

Benefits of **Zero-Voltage-Switching Topology**

VI Chip PRM Module

Simple to Use
- Point-of-load, Buck-Boost regulation
- Factorized Power Architecture
- Minimal external components

High Density
- Up to 1,700 W/in³, with 500 W in 1.1in² package

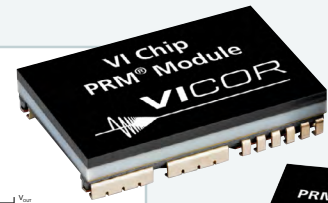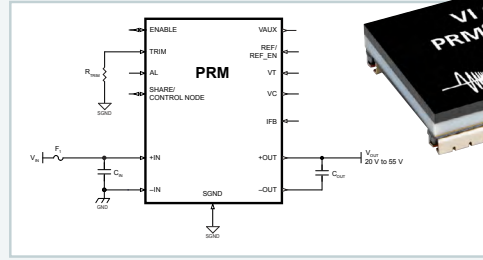## Wide Vin Optimized for 48 Vout
- 24 Vin, 18 – 36 Vin range
- 36 Vin, 18 – 60 Vin range
- 45 Vin, 38 – 55 Vin range
- 48 Vin, 36 – 75 Vin range

High Efficiency
- Full chip 500 W: 97.8%
- Half chip 250 W: 96.7%

Flexible
- Regulation: Remote sense, local loop, adaptive loop
- Parallel capabilities

PRM Modules Model Number	Input Voltage Nom. (V)	Range (V)	Output Voltage Voltage Range (V)	Output Power Max.	Output Current Max.	Package Size
P024F048T12AL	24 V	18 – 36 V	26 – 55 V	120 W	2.5 A	Full
P036F048T12AL	36 V	18 – 60 V	26 – 55 V	120 W	2.5 A	Full
P045F048T17AL	45 V	38 – 55 V	26 – 55 V	170 W	3.5 A	Full
P045F048T32AL	45 V	38 – 55 V	26 – 55 V	320 W	6.67 A	Full
P048F048T12AL	48 V	36 – 75 V	26 – 55 V	120 W	2.5 A	Full
P048F048T24AL	48 V	36 – 75 V	26 – 55 V	240 W	5.0 A	Full
PRM48BH480T200A00	48 V	38 – 55 V	5 – 55 V	200 W	4.17 A	Half
PRM48BF480T400A00	48 V	38 – 55 V	5 – 55 V	400 W	8.33 A	Full
PRM48AH480T200A00	48 V	36 – 75 V	20 – 55 V	200 W	4.17 A	Half
PRM48AF480T400A00	48 V	36 – 75 V	20 – 55 V	400 W	8.33 A	Full
PRM48BH480T250A00	48 V	38 – 55 V	20 – 55 V	250 W	5.21 A	Half
PRM48BF480T500A00	48 V	38 – 55 V	20 – 55 V	500 W	10.42 A	Full

These PRM modules can be further configured to meet your exact needs.

Resources

- ▶ Video: Overview of Vicor's VI Chip PRM Module
- 📄 PRM Product Information
- 🔧 Configure a PRM for your application's requirements
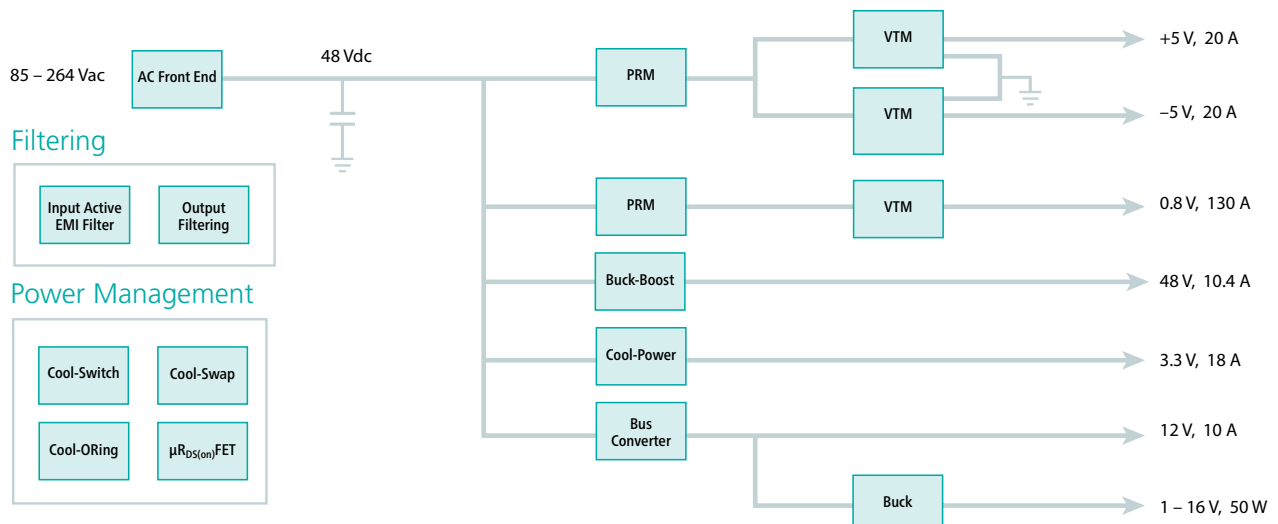
Solutions from **AC to Point of Load**

Introducing... The Growing ChiP Lineup
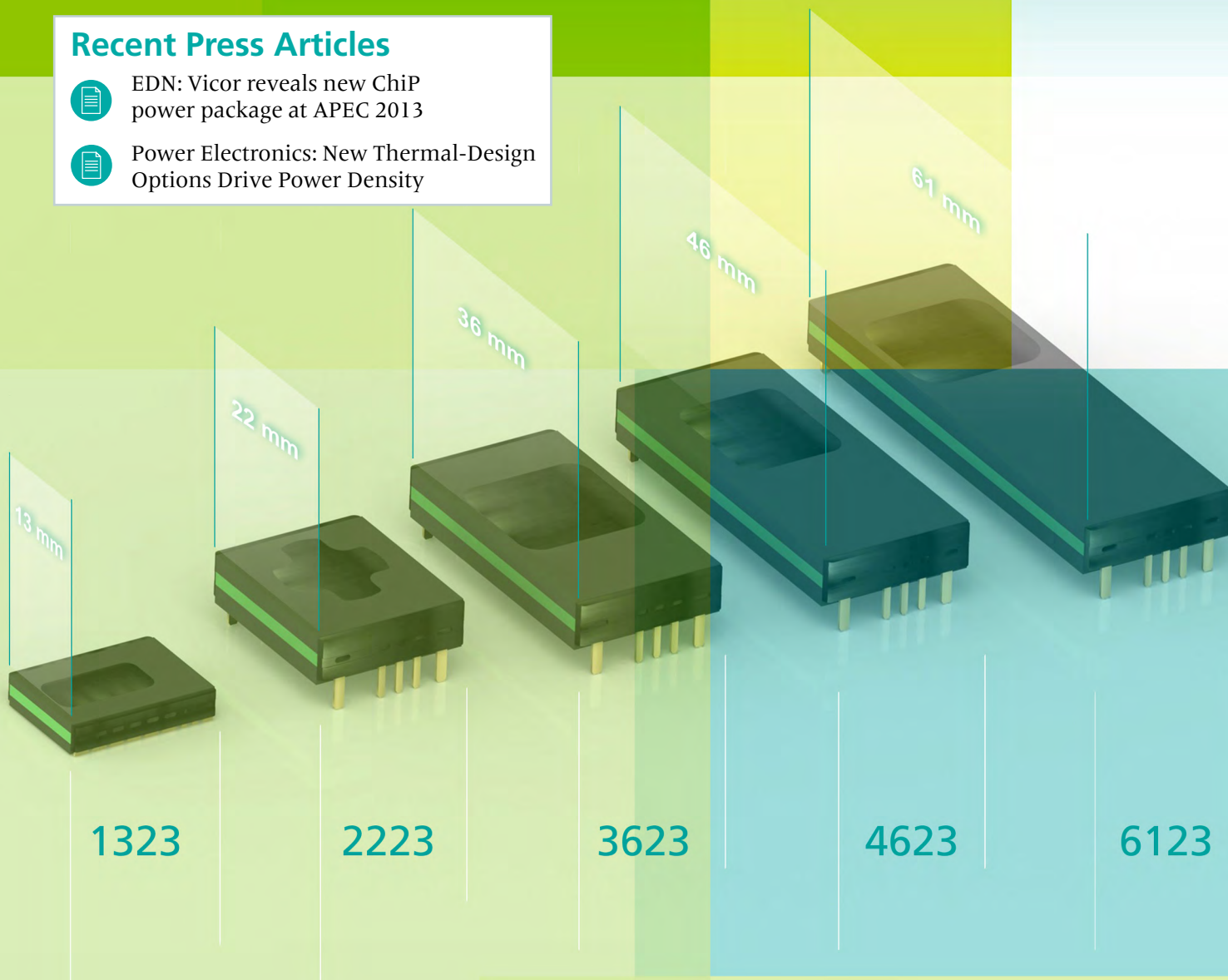
"Converters housed in Package" Technology

13 mm

22 mm

36 mm

46 mm

61 mm

1323

2223

3623

4623

6123

Resources

2013 APEC Plenary Session
Patrizio Vinciarelli, CEO, Vicor Corporation

Stephen Oliver
Vice President, VI Chip Product Line

▶ Vicor's CEO discusses ChiP technology at APEC

▶ An introduction to ChiP technology

Online Design Tools

Online Simulator

- Simulate electrical and thermal behavior
- User defines line and load conditions, input and output impedance and filters
- Simulations include start-up, steady state, shutdown, Vin step and load step, as well as thermal.
- Electrical and thermal performance showed in charts and tables

- Determine trim resistors for fixed and variable output voltage trimming
- Calculate required bus capacitance for VI-ARM, FARM, and ENMod modules
- Thermal calculator for heat sink selection

Filter Design

- Select attenuation and frequency
- Choose from five different topologies
- Supports regulated and unregulated converters

Design Calculators

Resources

- ▶ Video: Using Vicor's online simulator
- 🛠 Online simulator: VI Brick IBCs
- 🛠 Online simulator: BCMs
- 🛠 Online simulator: PRMs
- 🛠 Filter design tool
- 🛠 Design calculators

Calculation of Components for Parallel Damped Filter
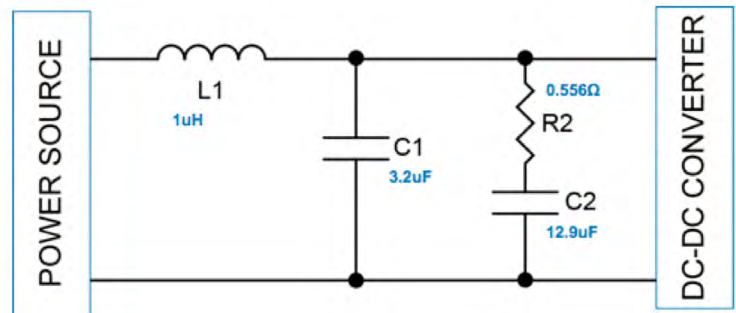
Configure Your Product

PowerBench™ online design center

- Design your own DC-DC converters to meet your application's requirements
- Or use hundreds of predefined designs
- Online registration allows designs to be saved

VI Chip® PRM® Module

- Point-of-Load Buck-Boost regulation with remote sense
- Full Chip (up to 500 W in 1.1 in^2)
- Half Chip (up to 250 W in 0.57 in^2)

Other DC-DC Converters

- Maxi, Mini, Micro Series: Full (160–600 W), Half (100–300 W), Quarter (50–150 W)
- VI-200 / VI-J00 Series: Full brick (50–200 W), Half brick (25–100 W)
- ComPAC, VIPAC Arrays and chassis-mount MegaMods

AC-DC Converters

- VIPAC - Autoranging input with filtering, multiple output, cold plate chassis,
- FlatPAC - Multiple output and autorange input with heat sink or conduction-cooled models

Complete power systems

- Westcor custom AC-DC
- High power density, small size, high efficiency
- Fan-cooled, slide-in assemblies

Resources

- 🛠 PowerBench online desisgn center
- 📄 Design calculators
- ▶ Webinar: Modeling, Simulation, and Selection Techniques in Power Design

Enabling Our Customers' Competitive Advantage

At Vicor, we enable customers to efficiently convert and manage power from the wall plug to point of load.

We master the entire power chain with the most comprehensive portfolio of high efficiency, high-density, power distribution architectures addressing a broad range performance-critical applications.

Vicor's holistic approach gives power system architects the flexibility to choose from modular, plug-and-play components ranging from bricks to semiconductor-centric solutions.

By integrating our world-class manufacturing and applications development, we can quickly customize our power components to meet your unique power system needs.

Focus Performance-Centric Markets / Applications

Communications

> 400 VDC Power Distribution
> Datacom
> Netcom
> Telecom Infrastructure

Computing

> Data Centers
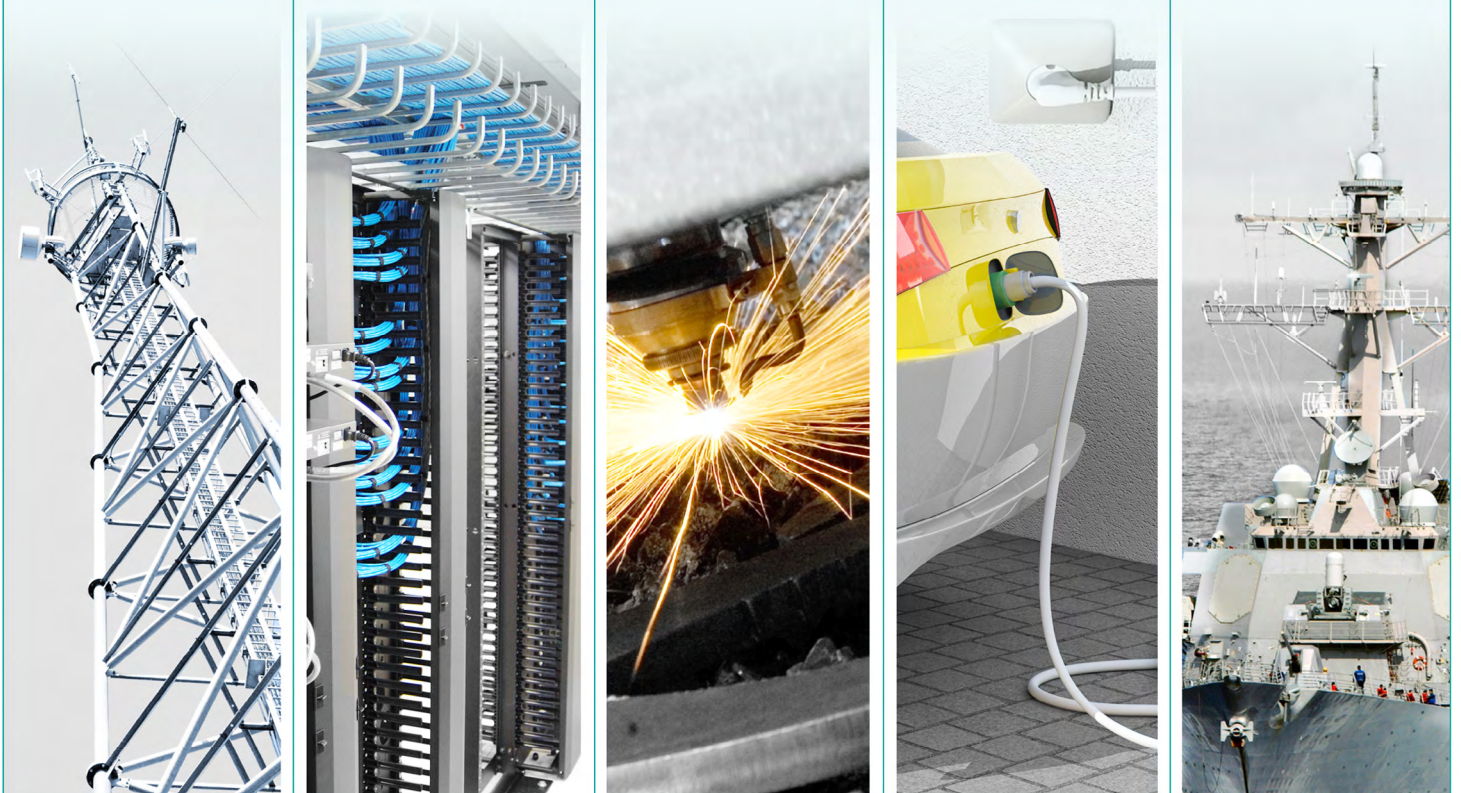> High Performance Computing
> Network Servers

Industrial

> ATE
> Lighting
> Process Control
> Transportation

Automotive

> Electric Vehicles
> Hybrid Vehicles

Defense/Aerospace

> Aircraft Test Equipment
> Ground Vehicles
> Radar
> Telemetry
> Unmanned Vehicles

Phone:
Europe: 00 800 8426 7000
US: 1 800 735 6200

designideas

ΣΔ isolation amplifier transfers low frequencies across barrier

by Francesc Casanellas

The isolation amplifier circuit of Figure 1 is simple but accurate. With the values shown it converts 0 to 5V DC or low frequency signals with unity gain, but you can adjust the gain by changing R4.

The lower half of Figure 1 is a DC to DC converter providing +12V and -5V to the isolated portion U1A and U1B. U2B through U2F is an oscillator and driver for Q1 which acts as a forward converter. The miniature transformer has been selected for its low interwinding capacitance, high primary inductance, and adequate leakage capacitance, which limits Q1's peak current. Because the frequency is high (about 300 kHz) and the primary inductance high (10 mH), the energy stored in the transformer is so low (15 mW avg.) that there is no need for snubber components, and Q1 itself clamps the overvoltage at turn off.

The isolation amplifier formed by comparator U1 works as a sigma-delta converter, with C4 as the integrating capacitor. The input voltage at J1 charges C4 through R4. When U1A's output goes low, C4 discharges to -5V through R1 and R2. D1 and R7 introduce a small hysteresis. When C4's voltage is below the hysteresis value, U1A output switches to a high level (open), C4 recharges again thorough R4 and the cycle starts again. The output pulse duty cycle varies relative to the level at J1. Due to

the negative feedback, the average pulsed output of U1A has to be the same as the input voltage since R1+R2 = R4.

U1B buffers the output and drives the optocoupler LED on when the output of U1A is low at -5V. U2A toggles following the same duty cycle pattern as U1, so the output average voltage filtered by R6 and C5 is the same as the average output of U1. The maximum linearity error is 1.3% from 5V to 0.2V. The switching frequency is about 3100 Hz at 4V, 1360 Hz at 0.4V, and goes down to 327 Hz at 90 mV. For increased accuracy at low input voltage, R2 and C1 mimic the delay in OC1, ensuring that the delays through the isolated and non-isolated parts are the same.

The circuit has been used in pH and Redox amplifiers, and to isolate the speed signal in three-phase AC inverters. If the input is both positive and negative relative to the isolated ground, you can use a circuit such as shown in Figure 2 to introduce a DC offset to U1A to always get a positive output.
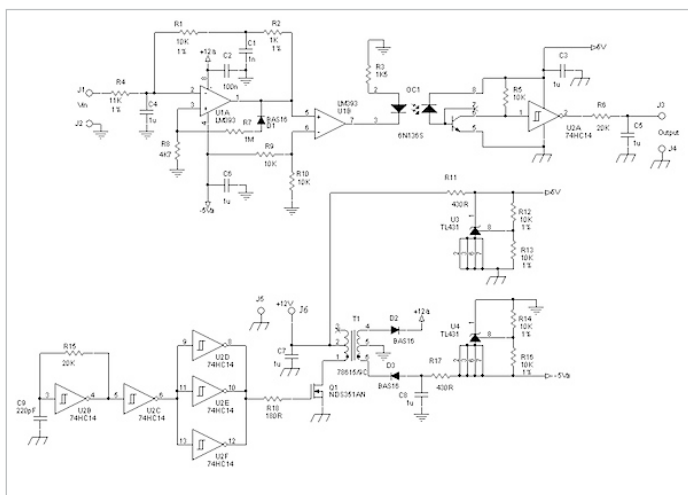
Figure 1 *The floating sigma-delta converter U1 generates a pulse train whose duty cycle depends on the voltage at J1 and J2. The filtered DC level is reconstructed at the output J3.*
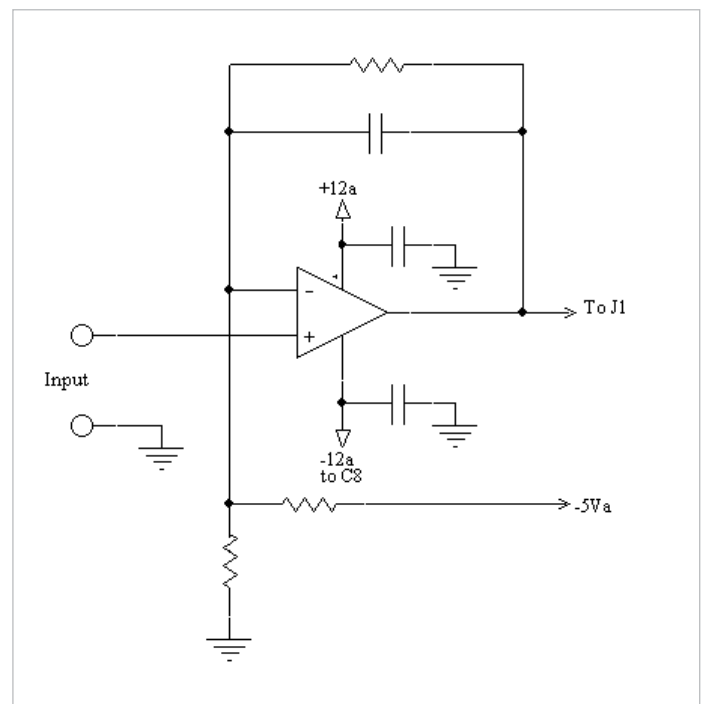
Figure 2 *You can use a generic level shifter to offset negative input levels (relative to J2) to positive-only at J1.*

designideas

Light-controlled oscillator uses solar cell junction capacitance

by sajjad Haidar

Any PN junction diode can be used as a variable capacitor in reverse biased mode, as well as in the forward biased mode before the knee voltage.

The capacitance is usually very small as the junction size is small. Though the varactor diode is specially designed for higher capacitance, it's still limited to a few hundred picofarads. A solar cell can also be used in some circuits as a variable capacitor. As its junction size is much larger than the usual diodes, much larger variation of capacitance is expected. There is a drawback using a solar cell as a capacitor: the reverse saturation current is also much higher, causing it to act like a leaky capacitor. Still, a solar cell can be used in some oscillator circuits to achieve a widely tunable frequency.

A Pierce oscillator was implemented using a BS170 MOSFET and a positive feedback network consisting of L1, C4, and C5. The amplifier gain was adjusted, choosing bypass capacitor C2 = 2 nF, for nearly sinusoidal output at an oscillation frequency around 250 kHz. A solar module (IXYS SLMD121H04, open circuit voltage: 2.52V; short circuit current: 50 mA) was connected in series with C8 (100 nF) to capacitor C5. When the solar-module capacitance (Csolar) varies, the series equivalent of Csolar and C8 paralleled with C5, also changes. The frequency of oscillation is given by the following equation:

$$\omega = \frac{1}{\sqrt{L\,C_T}}$$

$$\text{Where, } C_T = C_5 + 1 / \left[\frac{1}{C_{solar}} + \frac{1}{C_8} \right]$$

Two power LEDs (Bridgelux: BXRA-W0240) connected in series were used to illuminate the solar module, powered by a 24V variable power supply. The LEDs were mounted on a heatsink and were placed approximately 5 cm above the solar module. The whole area of the solar module (43 x 14 mm) was illuminated uniformly by the LEDs. Voltage across the solar module terminals was also measured at testpoint TP with changing illumination.

Initially, the solar module was put inside a small black box, and the voltage at TP read 6.2V, giving dark saturation current of 380 µA. Frequency of oscillation under darkness was 246kHz. With only ambient light, the frequency reduced to 245 kHz. As the LED current was increased, oscillation frequency continued going down; at 330 mA, the frequency was 116 kHz. Beyond a LED current of 330 mA, the total capacitance, CT, was not changing much, leaving the tuning range from 246 to 116 kHz. The tuning characteristic is shown in Figure 2.

The solar module capacitance was approximated by putting different capacitances in place of the solar module. In a separate test, short circuit current for the solar module was measured
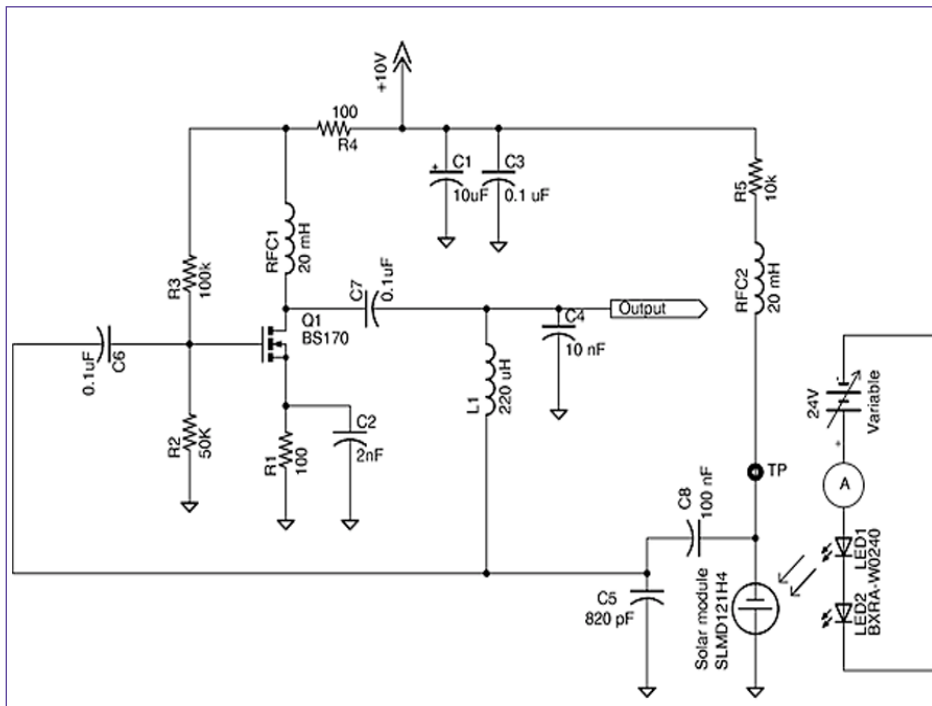
Figure 1: *Light-controlled Pierce oscillator*

Voltage (V)	Frequency (kHz)	Capacitance (nF)
6.1	246.1	1.45
5.86	245.4	1.5
5.8	244.7	1.6
5.21	240.2	1.8
3.11	221.8	3
1	190.7	4
0.55	181.6	4.7
0	169	6
-0.76	151.1	10
-1.46	134.51	22
-2.15	121	100
-2.24	119	470
-2.45	116	1000

Appendix 1: Solar cell capacitance

under illumination, keeping the same separation (approx. 5 cm). At 330 mA LED current, the corresponding short circuit current of the solar module was 14.5 mA; the light intensity was found from the data sheet of the solar module to be around 400 W/cm².

It should be mentioned that throughout the tuning range, the output amplitude varied as the closed loop gain varied due to changing capacitance and leakage in solar module. To achieve constant amplitude, an additional circuit would be needed.

REFERENCES:
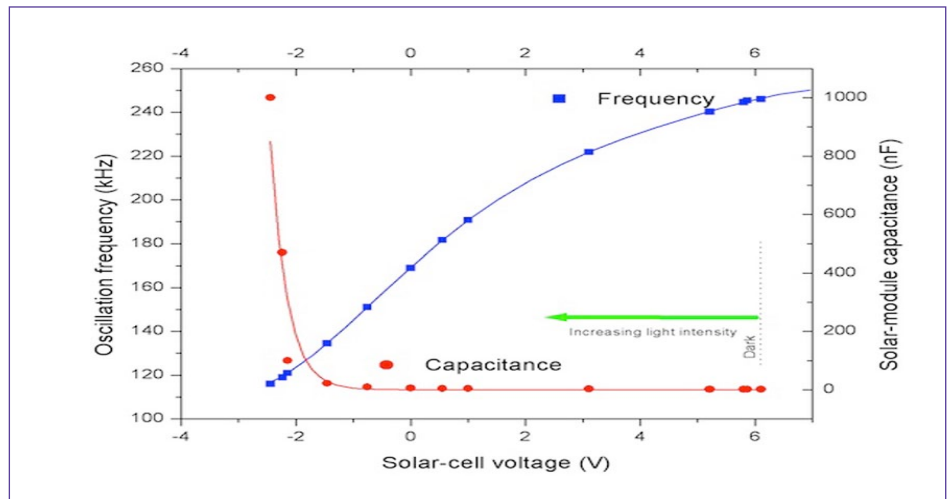1. G. Gonzalez, "Foundations of Oscillator Circuit Design", Artech House Inc., MA, USA, 2007.

Figure 2: *Solar cell voltage vs. capacitance & frequency*

# Adaptive Schmitt trigger tames unruly signals

by Michael Dunn

This design dates from around three decades ago; In biomedical instrumentation (for example), we're sometimes faced with very noisy or badly-behaved signals from which we need to derive information. In this example, I needed to "square up" a respiration signal, which can exhibit wide variations in amplitude and frequency, along with a wandering baseline. Presented here is an adaptive "super-Schmitt," with many adjustable parameters, that did an extremely good job of taming the input signal.

The design values here are tweaked for an expected input range of 50 mV to 1V P-P and 0.07 Hz to 2 Hz.

U1 & U2 detect the positive & negative peaks of the input, but unlike typical detectors, include R1 and R2 to provide damping (spike rejection) as required, dependant on the signal characteristics. These networks, in conjunction with R16, determine how quickly the held peaks decay. The P-P amplitude tracked by these detectors (buffered by U3 and U4) is used to both adjust the hysteresis band of the final comparator U6, and to provide a zero-crossing reference.
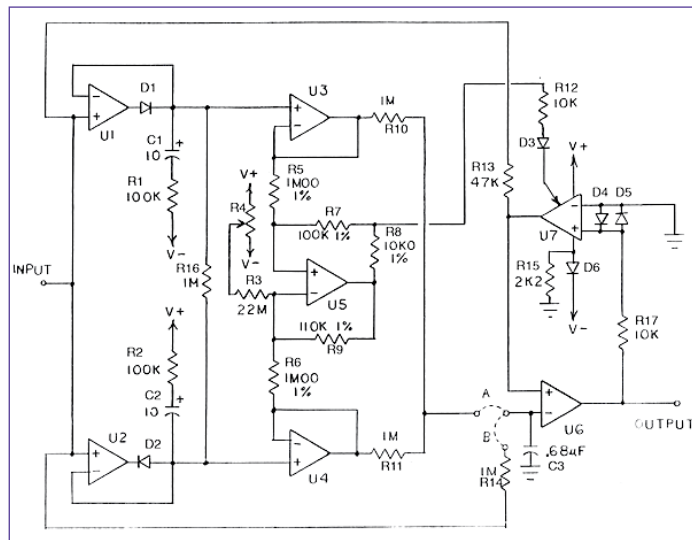
Hysteresis adjustment is accomplished by operational transconductance amp (OTA) U7. This chip (originally a 3080, but a more modern part like the LM13700 should work too) basically multiplies its differential input voltage by the unipolar bias current (the arrow input) to derive its output current. In this case, by saturating the input (0.7V

is enough), the OTA acts more like a polarity reversal switch, which mirrors the bias current to the output, either sourcing or sinking depending on the differential input polarity. The output current develops a voltage across R13 which adds to or subtracts from the input signal depending on the circuit's digital output, thus providing hysteresis. U5 implements a differential-input current-to-voltage converter for driving the OTA's bias input (which is internally referenced to the negative supply rail). U6, the final output comparator, compares the input signal, ±hysteresis to either the low-pass-filtered midway point between the signal peaks (jumper "A"), or to a low-passed version of the signal itself (jumper "B"). This is chosen based on your signal's characteristics; I found "A" worked best in my application.

The trimmer, R4, sets the quiescent hysteresis and compensates for any amp offsets. D6 puts U7's bias input within the output range of the op-amps I used, and could be removed or modified depending on your op-amps and OTA. Supplies are assumed to be clean and stable.

The astute reader will ask why I didn't do the obvious, and use an OTA in place of the U5 VCCS circuit. Unfortunately, 30 years after the fact, I'm not quite sure. There may have been a reason. Is this circuit still useful today? I'll claim it is, though like many such circuits, a microcontroller could do a good job too. Take your pick.

REFERENCES:
Jung, W.G., IC Op-amp Cookbook, section 4.2.4: Bi-directional output VCCS

productroundup

Ultra-miniature crystal package with 0.5mm profile

IQD Frequency Products' IQXC-42 quartz crystal measures 2.0 x 1.6mm with a height of only 0.5mm. The new ultra-miniature model is especially suitable for many portable applications; the crystal is available in frequencies between 20 MHz and 50 MHz and operates over the full industrial temperature range of -40 to +85C. Frequency stabilities can be specified as low as ±10ppm over commercial temperature ranges. In line with the requirements of the latest generation of microprocessors the load capacitance can be as low as 8pF. Housed in a 4-pad ceramic package with a hermetically sealed metal lid which helps to minimise EMI radiation, the product is designed to able to withstand shock levels of up to 1000G in accordance with IEC 60068-2-27.

IQD; www.iqdfrequencyproducts.com

6 GHz envelope and RMS power detector

Analog Devices' ADL5511 is an RF envelope and RMS detector that uses ADI's TruPwr technology. The envelope output voltage is presented as a voltage that is proportional to the envelope of the input signal. The rms output voltage is independent of the peak-to-average ratio of the input signal. The RMS output is a linear-in-V/V voltage with a conversion gain of 1.9 V/V RMS at 900 MHz. The envelope output has a conversion gain of 1.46 V/V at 900 MHz and is referenced to an internal 1.1V reference voltage, which is available on the EREF pin. The ADL5511 can operate from DC to 6 GHz on signals with envelope bandwidths up to 130 MHz. The extracted envelope can be used for RF power amplifier (PA) linearisation and efficiency enhancements and the RMS output can be used for RMS power measurement. The ADL5511 operates from −40°C to +85°C and is available in a 16-lead, 3 × 3 mm LFCSP package.
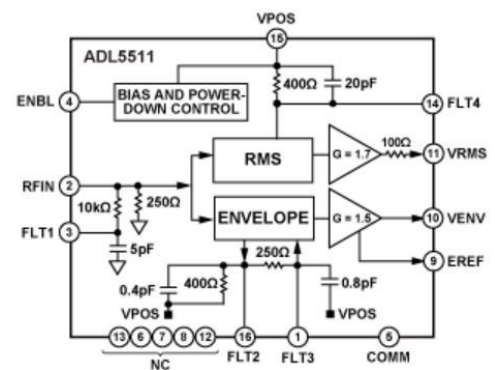
Get the data sheet from Analog at; www.analog.com/static/imported-files/data_sheets/ADL5511.pdf

Smart high-side switches for 24V systems

Infineon has introduced a series of pin-compatible single-channel 24V high-side switches in its PROFET+ 24V family, in DSO-14 EP packages and with embedded diagnostic and protective functions. The power transistor in the BTT6020-1EKA, BTT6030-1EKA, and BTT6050-1EKA is an N-channel vertical power MOSFET with charge pump. The devices are designed to drive lamps as well as LEDs in the harsh automotive environment, in particular the 24-V on-board systems of trucks and other heavy vehicles. The high current sense accuracy is able to diagnose even the smallest loads, such as LEDs. The devices feature high short-circuit robustness, specified at a minimum of 100k SC cycles. You can use the parts with grounded 24V loads, and diagnostic feedback is available to a microcontroller; you can switch all types of resistive, inductive and capacitive loads including loads with high inrush currents. The parts are AEC qualified, operate over 5-36V and have a standby current under 0.5µA. They are ESD protected and have PWM capability up to 500Hz, with very low leakage current in the OFF state. Logic inputs are 3.3V and 5V compatible.

Infineon; http://www.infineon.com/

LED driver targets backlighting

Advanced Power Electronics' APE1612-3 is a step-up converter capable of efficiently driving up to eight white LEDs in series for backlighting applications. It uses a current mode, 1.2 MHz fixed frequency architecture to regulate the LED current, which is set using an external current sense resistor. The APE1612-3 features a 300mV feedback voltage that reduces power loss and improves efficiency. The OV pin monitors the output voltage and turns off the converter if an over-voltage condition is present due to an open circuit condition. The APE1612-3 includes under-voltage lockout, current limiting and thermal shutdown protection preventing damage from an output overload. A wide 200Hz to 200kHz range enables the device to be used in PWM dimming. It comes in a TSOT-26 package.

Advanced Power Electronics; www.a-powerusa.com/docs/APE1612-3.pdf

Freescale Kinetis E series MCUs in IAR toolchain

IAR Systems now has support for the efficient, recently introduced Kinetis E series microcontrollers. The support is available using IAR Embedded Workbench for ARM, which is a complete set of high-performance tools for embedded development. Kinetis E series microcontrollers (MCUs) are aimed at white goods and industrial applications – equipment commonly operating in high-noise environments. These first 5V, 32-bit MCUs built on the ARM Cortex-M0+ processor feature rugged electromagnetic noise immunity for systems historically limited to 8- and 16-bit MCUs, while providing high efficiency and optimal code density. IAR Embedded Workbench generates efficient and reliable flashable code for Kinetis microcontrollers. It is integrated with Freescale MQX Software Solutions and with Freescale Processor Expert software modelling tool and comes with example projects for MQX, the Tower kit, and the Freedom Development Platform. It offers automatic project configuration for all Kinetis devices.

IAR; www.iar.com/kinetis.

TVS diodes protect avionics from lightning

Microsemi has announced two plastic large area device (PLAD) transient voltage suppression (TVS) diode products; the 6.5 kW and 7.5 kW devices are the latest addition to Microsemi's PLAD TVS product portfolio and feature 50% smaller footprints than the company's current 15 kW and 30 kW (pictured) solutions. The new TVS diodes are offered in voltages ranging from 10V to 48V and comply with industry-standard RTCA DO-160 requirements for lightning protection in aircraft.
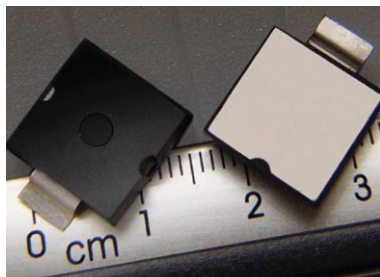
Features include Microsemi's low-profile PLAD surface mount package, which allows product developers to reduce board space and overall component weight. The highly-integrated, single-component diodes are also more reliable than alternative multiple-device solutions, making them suitable for demanding aviation, military, automotive and industrial applications. Microsemi's TVS diodes provide aircraft electrical systems with critical protection by going into avalanche breakdown within no more than a few nanoseconds after a strike, clamping the transient voltage and routing its current to the ground. The 6.5kW and 7.5kW series TVS diodes are priced at $2.49 (10,000).

Microsemi; www.microsemi.com/product-directory/606-discretes

Automotive ISO26262 safety-compliant LIN transceiver

ams says its AS8530 is the first miniature power/transceiver IC to support LIN slave applications, which also complies with the ISO26262 functional safety standard. The AS8530 is a power management and communication device that includes a LIN 2.1 transceiver, a 50-mA LDO to supply a local MCU and a reset generator, in an 8-pin SOIC 8 package. AS8530 also offers a series of system management functions through a shared pin serial interface, all within an 8-pin SOIC8 package. The addition of enhanced diagnosis functions provides built-in support for the requirements of ISO26262. A two-wire serial port routed through shared Enable and TX pins allows the device to read out status registers and provide diagnosis information, for ISO26262-compliant systems, which must be able to cease operation safely when in a fault condition. The chip also offers a reset generator and an output voltage monitor and has a unique chip ID to support traceability requirements. The AS8530 LIN IC costs $2.21 (1,000). An evaluation kit for the interface IC AS8530, the AS8530 adapter board, is available online, priced at $70.

ams; www.ams.com/Interface/LIN-Bus-System/AS8530

48-V battery, HV brushless DC motor driver

The A4900 from Allegro MicroSystems Europe is a high-voltage (600V) MOSFET gate-driver IC designed for driving brushless DC motors in EVs and HEVs, and in 48V automotive battery systems such as electronic power steering, air-conditioning compressors, fans, pumps and blowers. The A4900 is also available in a non-automotive version for high-voltage industrial and commercial applications. The device incorporates six gate drives capable of driving a wide range of N-channel IGBT or power MOSFET switches. The gate drives are configured as three high-voltage high-side drives and three low-side drives. The high-side drives are isolated by up to 600V to allow operation with high bridge (motor) supply voltages, and use a bootstrap capacitor to provide a voltage higher than the supply gate drive voltage needed for N-channel FETs. Each FET can be controlled with a TTL logic level input compatible with 3.3V or 5V logic systems. Integrated diagnostics provide indication of under-voltage, over-temperature and power bridge faults, and can be configured to protect the power switches under most short-circuit conditions. Detailed diagnostics are available in the form of a serial data word. The A4900KLQTR-T is supplied in a 44-lead QSOP (suffix 'LQ') package.

Allegro Microsystems; www.allegromicro.com/en/Products/Motor-Driver-And-Interface-ICs/Brushless-DC-Motor-Drivers/A4900.aspx

productroundup

## High-frequency, power film resistors

Riedon has expanded its range of specialist resistive solutions with a power resistor design that is non-inductive and achieves superior performance in high-frequency applications and high-speed pulse circuits. The product series provides devices that offer excellent thermal resistance in small-size, thin-profile TO-style packages for high-density applications. The package configurations available cover power ratings from a few Watts up to 600W in both through-hole and surface mountings: These start with the PF1260 series in an epoxy-moulded TO-126 leaded package, with resistances in the range 0.01Ω to 51 kΩ, tolerances from ±1%, a temperature coefficient (TCR) from ±50ppm and provide up to 20W dissipation (with a heatsink). The PF2200 and PF2470 series offer a similar specification but with dissipation up to 50W and 140W respectively in leaded TO-220 and TO-247 packages. PF2270 series uses the screw-terminal TO227 style package to handle up to 300W. The low-inductance design makes these parts suitable for high frequency applications, such as wireless communications, or in systems that need to withstand short-duration, high-energy pulses, for example, medical equipment.
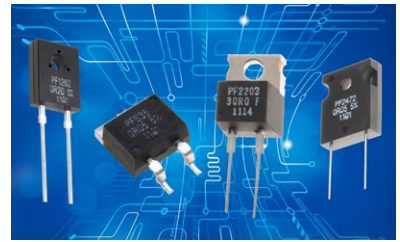
Riedon's (www.riedon.com) range of TO-style power resistors is available from Digi-Key (www.digikey.com)

I²C voltage level translation for DDR4 at 1 MHz
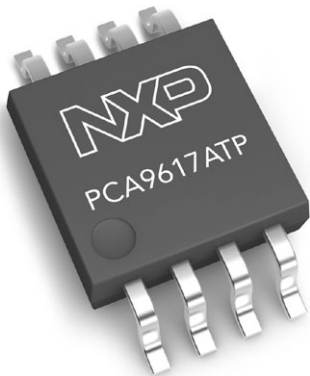
A bidirectional voltage I²C-bus translation buffer is intended for application in areas such as high-performance servers. The PCA9617A Fast-mode Plus (Fm+) I²C-bus buffer from NXP is designed for emerging server applications that use DDR4 SDRAM memory. This voltage-translating bus buffer allows you to design next-generation server systems using new DDR4 technology with the I²C-bus operating at up to 1 MHz, and voltage level translation of 0.8V on the CPU side to 2.5V on the SDRAM module side. The PCA9617A is the first Fm+ device specifically designed for servers. It operates up to 1 MHz with normal Fast-mode drive to allow operation on more heavily capacitive loaded buses, but is backward-compatible to Fast-mode and Standard-mode speeds. It is a CMOS integrated circuit that provides voltage level shifting between 0.8V and 2.5V supply voltages for Fast-mode plus I²C-bus or SMBus applications. While retaining all the operating modes and features of the I²C-bus system during the level shifts, it also permits extension of the I²C-bus by providing bidirectional buffering for both the data (SDA) and the clock (SCL) lines, one bus, split into two sections of 550 pF (max) at 1 MHz.

NXP Semiconductors; www.nxp.com

650-V automotive MOSFETs in TO-247

STMicroelectronics says its STW78N65M5 and STW62N65M5 are the industry's first 650V AEC-Q101 automotive-qualified MOSFETs in the TO-247 package. The 650V rating provides greater safety margin when exposed to high-voltage spikes, enhancing the reliability of automotive power and control modules. The two devices' extremely low on-resistance (RDS(ON)) of 0.032Ω and 0.049Ω respectively, combined with the compact TO-247 outline, enhances system energy efficiency and power density. The new devices owe their performance to ST's MDmesh V super-junction technology, which produces high-voltage devices with very low RDS(ON) per die area allowing smaller package sizes. Gate charge (Qg) and input capacitance are also low, resulting in outstanding Qg x RDS(ON) figure of merit (FOM) with high switching performance and efficiency. In addition, superior avalanche robustness ensures increased ruggedness at sustained high-voltage operation. Prices are from $8.95 for the STW62N65M5 and $9.75 for the STW78N65M5 (1000).

ST; www.st.com/mdmeshv

AMD lowers G-Series APU power

AMD has announced a low-power Accelerated Processing Unit (APU) in its G-Series SOC family with the GX-210JA, further reducing x86 power requirements for embedded designs. The GX-210JA APU, a full System-on-Chip (SoC) design, uses one-third less energy than the previous low-power Embedded G-Series SOC product while providing full graphics capabilities. At only 6W maximum thermal design power (TDP), and approximately 3W expected average power, the GX-210JA is part of the AMD Embedded G-Series SOC processor family that offers enterprise-class Error-Correction Code (ECC) memory support; industrial temperature range of -40°C to +85°C; availability with dual- or quad-core CPUs; an AMD Radeon GPU; and integrated I/O controller.

AMD; www.amd.com/us/products/embedded/processors/Pages/g-series.aspx
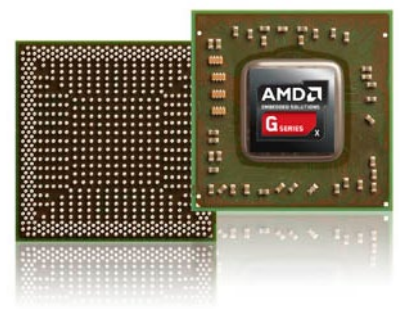
Disappearing data
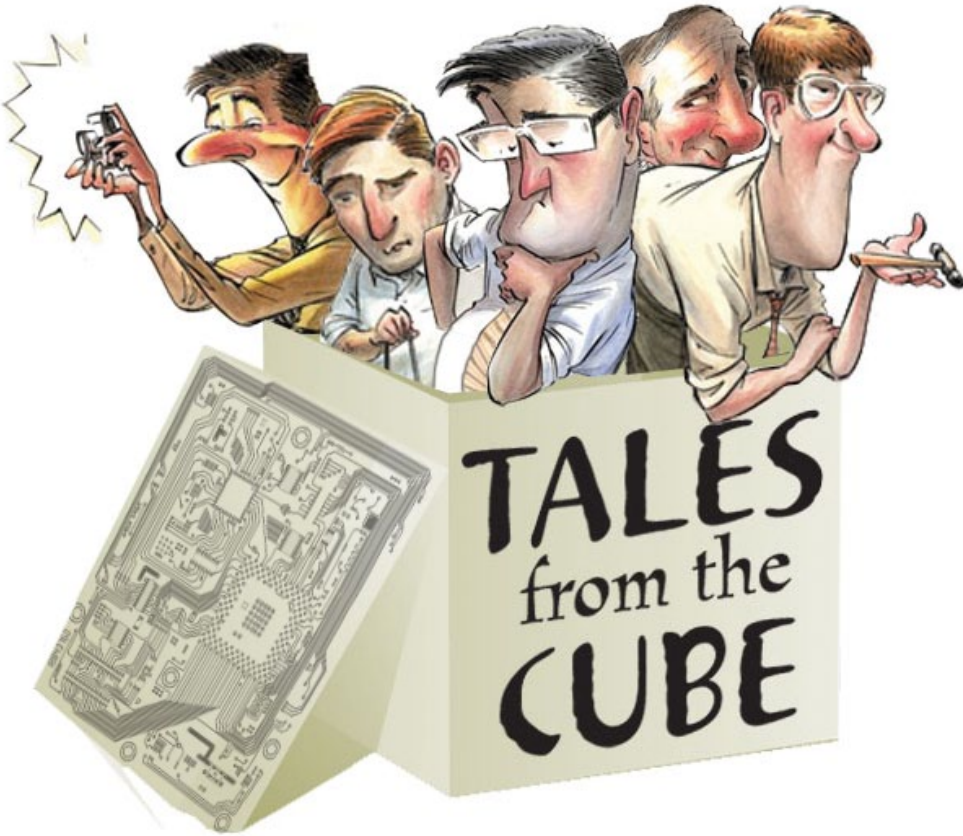
My boss once told me that finding and fixing someone else's software bugs is worse than fixing your own. He was right.

Years later, I was working as a project engineer for another company. I had my own developing project and very little to do with the old products that were well settled in production. One day a customer called and said a meter he just bought was not working. The needle won't move. Older units he had from years before were still fine. And then another customer called, and another with the same problem.

Since these units were powered by a 9V battery, we asked the customers to replace the battery. Nothing. A few other attempts to "press this" and then "press that" also failed, so we had the meters sent back.

Initial evaluation showed that the customers were right; the meters were not working. Upon recalibration though, they worked just fine. Although production records showed the units had been originally calibrated, it was decided that it was just a quality control problem. The units were all recalibrated and shipped back to the customers.

But then about half of the customers complained again about the same problem. Now it was obvious that somehow the calibration data was lost. And that's when engineering got involved and my problems started.

The bad news was that the product had been designed years ago by an external consultant and little data or tools were available. I had the code, but no emulator or development system, so how would I debug? With just a needle indicator, no data communication, and no display, there was no way to read the calibration data, and no way to put in a breakpoint and check the trace buffer.

Luckily, there was an LED on board. My first guess was that the calibration routine ran randomly and overwrote my good data, so I modified the code to have the LED blinking only when the Write_to_EEprom() function was executed.

I programmed a unit and started to play with it. I let it soak at +55°C and then at −40°C. I let it sit overnight in a humidity room. I gently dropped it. I pressed the buttons in crazy combinations and still no accidental calibration. I then removed the battery and reinserted it in the slot.

Eureka! My red LED started to blink. And sure enough, after I pressed the "measure" button, nothing happened. All my calibration data was gone, and my experiment was repeatable.

What happened? The phenomenon was relatively recent, only after the original (obsolete) 9V connector was replaced with a different one. The original connector would have you connect one polarity first, and then the other, so the connection to the power was "clean." The new one was rigid and had both + and − connect at the same time, which would sometime require several tries to get it all the way in.

The circuitry was designed in such a way that Vdd was applied to the micro as soon as the battery was connected and no delay circuit was designed in to allow for voltage to settle. Nor was there an "ON" button to enable the power to the microcontroller. The voltage bounce generated as the battery was plugged into the new connector would drive the micro crazy in absence of a brown-out detector, and would sometimes jump to the save_calibration() routine, overwriting data with zeros.

Now that I knew what the problem was, the next step was to solve it. Any hardware change was out of the question; time was critical, production was on hold, and the company could not afford the time or cost to redesign the board. So it must be software.
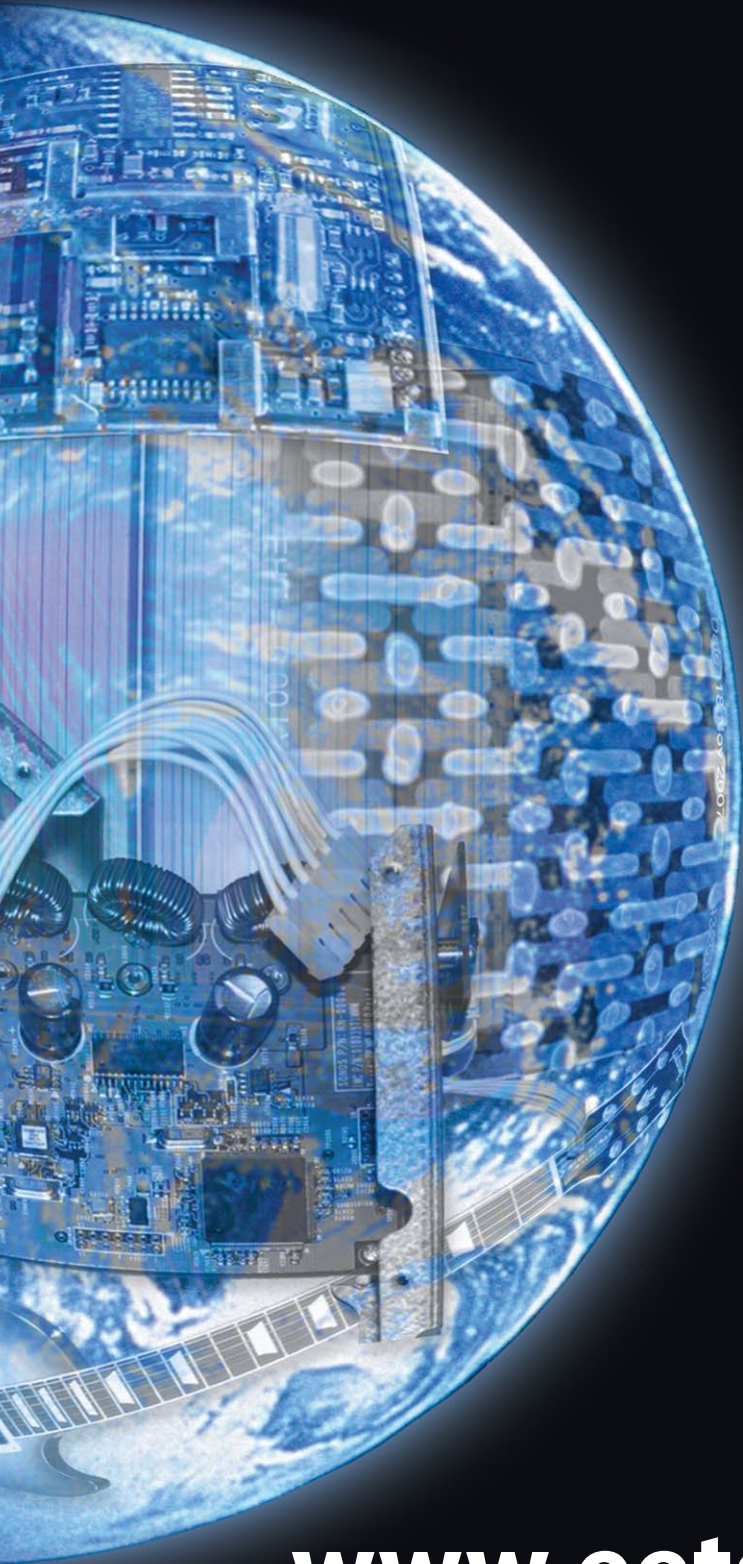
I defined a new variable do_the_calibration, initialized with zero. The variable was set only when a "valid" calibration was initiated and not all the calibration data was zero. In my Write_to_EEprom() routine, I checked the variable right before the "Write" command was to be sent to the eeprom device, and allowed the write only if do_the_calibration was set. After the write, the variable was cleared again. With this new firmware, the meter would still attempt to write the eeprom when the battery was connected, but the protection was there and never allowed it.

So simple, right?

Mihaela Costin is a senior electrical engineer at Curtis Instruments.